

Critical Benchmarking of the G4(MP2) Model, the Correlation Consistent Composite Approach and Popular Density Functional Approximations on a Probabilistically Pruned Benchmark Dataset of Formation Enthalpies

Sambit Kumar Das,¹ Sabyasachi Chakraborty,¹ and Raghunathan Ramakrishnan^{1, a)}
 Tata Institute of Fundamental Research, Centre for Interdisciplinary Sciences, Hyderabad 500107,
 India

(Dated: 22 August 2022)

First-principles calculation of the standard formation enthalpy, ΔH_f° (298K), in such large scale as required by chemical space explorations, is amenable only with density functional approximations (DFAs) and some composite wave function theories (cWFTs). Alas, the accuracies of popular range-separated hybrid, ‘rung-4’ DFAs, and cWFTs that offer the best accuracy-vs.-cost trade-off have as yet been established only for datasets predominantly comprising small molecules, hence, their transferability to larger datasets remains vague. In this study, we present an extended benchmark dataset of over two-thousand values of ΔH_f° for structurally and electronically diverse molecules. We apply quartile-ranking based on boundary-corrected kernel density estimation to filter outliers and arrive at Probabilistically Pruned Enthalpies of 1908 compounds (PPE1908). For this dataset, we rank the prediction accuracies of G4(MP2), ccCA and 23 popular DFAs using conventional and probabilistic error metrics. We discuss systematic prediction errors and highlight the role an empirical higher-level correction (HLC) plays in the G4(MP2) model. Furthermore, we comment on uncertainties associated with the reference empirical data for atoms and the systematic errors stemming from these that grow with the molecular size. We believe these findings to aid in identifying meaningful application domains for quantum thermochemical methods.

Keywords: thermochemistry, composite wave function theory, density functional theory, enthalpies of formation

I. INTRODUCTION

An unmet promise in ab-initio quantum chemistry is to predict molecular and reaction enthalpies with such high an accuracy, that reaction energies and relative stabilities of constitutional/conformational/geometric isomers can be established in agreement with experimentally observed trends—but at a computational cost that is comparable to that of a density functional approximation (DFA) with a reasonably converged basis set^{1,2}. This situation is apparent in the context of emerging data science campaigns, where computational explorations and statistical inference of molecular properties across *chemical compound space* is the prime focus^{3–8}. Arguably, one of the most sought-after molecular properties for data-mining is the standard formation enthalpy, ΔH_f° (298K), because of its significance to energetics and rates of industrial^{9,10} and atmospheric chemical reactions^{11,12}. Hence, development of a rapid thermochemistry protocol demonstrating a faithful transferability of accuracy from that of molecules used for the method’s benchmarking (*i.e. training*) to a query molecule—with arbitrary stoichiometry/valency and non-standard bond distances/angles—will remain an active research domain^{13–15}.

Karton classified the most widely used composite

wavefunction theories (cWFTs) into those involving a post-CCSD(T)-level energy correction and those requiring a CCSD(T)-level treatment¹⁶. The former includes: W4¹⁷, HEAT-345QP¹⁸, and HEAT-456QP¹⁹ which depend on higher-order terms in the coupled-cluster expansion (*i.e.* quadruple, quintuple and higher excitations) to forecast molecular energies of ‘high chemical accuracy’, with prediction error ≤ 1 kJ/mol^{20,21}. Alas, the severe computational complexities of these methods restrict their applicability to small molecules with at most a few dozen electrons. The latter category of thermochemistry methods is dependent on electron correlation energy estimated only at the CCSD(T)-level, where the triples contribution is included perturbatively. Such a compromise extends the application domain of this class of methods—for instance, CBS-QB3²², G4²³, ccCA^{24–26} and their offshoots—to somewhat larger molecules with up to a couple of dozen main group atoms. Depending on the size of the basis set with which the CCSD(T) energy is estimated, cWFTs can yield an average prediction accuracy in the $\approx 1 - 2$ kcal/mol range¹⁶. However, it must be noted that based on the computational complexity of these methods which scale unfavorably with molecular size, their application domain is restricted to molecules of size CF₄ or CH₃COOH for FCI/CBS based methods, C₆H₆ or C₆H₁₄ for CCSDT(Q)/CBS based methods, C₂₀H₂₀ for CCSD(T)/CBS methods, while CCSD(T)/TZ based methods can handle large systems like C₆₀.

A number of data-driven computational chemistry

^{a)}Electronic mail: ramakrishnan@tifrh.res.in

benchmark studies have explored subsets of the GDB17 molecular universe²⁷ comprising 166,443,860,262 (*i.e.* 166.4 billion) closed-shell, organic molecules each containing up to 17 atoms of C, N, O, S, and halogens. These high-throughput computational studies have catered the data requirements of methodological studies focusing on machine learning (ML) modeling^{28,29}. For instance, a past study has computed DFT-level structures and properties of a small subset of the GDB17 dataset with 133,885 small organic molecules (the QM9 dataset) each containing up to nine C, O, N and F atoms^{30,31}. Recently, the QM9 dataset was subjected to rigorous G4(MP2) calculations reporting total energies, atomization energies and standard enthalpies of formation^{5,32}. Other studies^{33,34} have extended these works by applying ML and Δ -ML³¹ to statistically infer G4(MP2)-level energies of a small set of organic molecules containing more than 9 heavy atoms. On the basis of dataset size alone, these studies represent some of the massive high-throughput quantum chemistry efforts ever undertaken. However, it remains to be seen if these ΔH_f° values predicted with G4(MP2) for the QM9 dataset will be quantitatively accurate to a degree that is relevant for comparison with experiments.

The complexity involved in validating computed results in chemical space explorations is twofold: Firstly, it is a non-trivial task to automate the collection and pruning of available experimental energies for such a large dataset as QM9. Secondly, even if all these molecules are ‘synthetically feasible’, only a tiny fraction have been plausibly characterized by gas phase measurements. Seemingly, the only viable way of probing the transferability of a computational method to unexplored regions in the chemical space is to benchmark on compounds of similar chemical composition. In this context, Narayanan *et al.*⁵ selected experimental values of ΔH_f° for 459 closed-shell hydrocarbons and their substituted analogues, containing atoms similar to those in the QM9 dataset, from Pedley’s extensive compilations^{35,36} and observed an average prediction error of 0.8 kcal/mol for G4(MP2). This value is comparable to that of G4(MP2)’s³⁷ and ccCA’s³⁸ mean errors noted for similar molecules in the G3/05 small molecules dataset³⁹. However, such high prediction accuracies are not expected to hold for electronically and structurally more diverse molecules that can be combinatorially generated from the QM9 set by protonation, deprotonation, or isovalence-electronic substitutions. For instance, Schwilk *et al.*⁴⁰ have selected about 4,000 molecules from the QM9 set and derived from this subset a new dataset QMspin, comprising 8000 triplet and 5000 singlet carbene compounds. To gain insight on the applicability of G4(MP2) to such non-trivial chemical subspaces, it is a timely pursuit to benchmark widely employed cWFTs on larger, curated benchmark datasets by extending upon existing thermochemistry benchmark sets.

In this study we aim to: (i) collect reference ΔH_f°

values from several previous reports, include to these new benchmark datasets containing experimental results and present a consolidated dataset with $\approx 2k$ entries, (ii) apply a probabilistic procedure based on the best theoretical method applicable to the entire set to detect and eliminate potential outliers in the dataset, (iii) report on the prediction errors based on mean and percentiles metrics for the cWFTs, G4(MP2) and ccCA along with 23 popular DFAs and 2 semi-empirical methods, (iv) analyze the critical role of the HLC in the performance of G4(MP2) and comment on the method’s transferability, (v) from the larger dataset presented, identify and study a new benchmark set with isomerization reaction enthalpies for 24 sets of constitutional isomers, and (vi) finally, inspect the uncertainties in thermochemistry calculations arising due to the use of empirical reference data for atoms.

II. COMPUTATIONAL DETAILS

G4(MP2), ccCA and DFAs-level thermochemistry calculations were automated through *in-house* scripts which rely on the ORCA suite of programs^{41,42}. PM6⁴³ and PM7⁴⁴ calculations were done via the MOPAC suite of programs⁴⁵. We considered 23 DFAs from various levels of Perdew’s ‘Jacob’s ladder’⁴⁶, generalized gradient approximation (GGA): BLYP⁴⁷, PW91⁴⁸ and PBE⁴⁹; hybrid GGA: B3LYP⁵⁰, O3LYP⁵¹, X3LYP⁵² and PBE0⁵³; meta-GGA: TPSS⁵⁴; hybrid meta-GGA: TPSS0⁵⁵ and M062X⁵⁶. We also selected the range-separated hybrid functionals: CAM-B3LYP⁵⁷, ω B97X⁵⁸, ω B97X-D3⁵⁸, ω B97X-V⁵⁹, ω B97M-V⁶⁰, ω B97X-D3BJ, and ω B97M-D3BJ, where Grimme’s D3 dispersion with Becke-Johnson damping (D3BJ)^{61–64} has been included explicitly. Furthermore, B2PLYP⁶⁵, B2PLYP-D3⁶⁶ and mPW2PLYP-D⁶⁷ represent the double-hybrid functionals considered in this study, some of which include dispersion corrections. Additionally, we also benchmarked a few of the aforesaid functionals with an additional dispersion correction, namely, B3LYP-D3, TPSS0-D3 and M062X-D3.

Initial geometries for molecules from previously studied datasets were collected from their corresponding sources—when such information was available—and subjected to geometry relaxations. For compounds with no previously reported geometries, we consulted the popular online chemical databases: NIST⁶⁸, ChemSpider⁶⁹ and Pub-Chem⁷⁰. In some cases, we created initial geometries using the software Avogadro⁷¹ and performed minimum energy geometry relaxation with universal forcefield (UFF)⁷². We performed all DFA calculations at the B3LYP/6-31G(2df,p) minimum energy geometry in a single point fashion using the def2-QZVP basis set, that has been shown to yield predictions close to the Kohn-Sham limit⁷³. PM6 and PM7

calculations were performed using precise geometry relaxation thresholds at the corresponding levels. Geometry optimizations with DFAs were carried out with tight convergence criteria with 10^{-4} as the threshold for the maximum component of the force vector. To facilitate convergence of the geometry towards the energy minimum, force constants were computed at every fifth step of geometry optimization. In all calculations, SCF convergence was reached with `verytightscf` criteria corresponding to a threshold of 10^{-9} Hartree for the electronic energy. For the numerical quadrature of the exchange correlation part of the energy in DFAs, we used Lebedev-434 angular grids and Grid7 settings for Gauss-Chebyshev radial grids. From the zero-point corrected electronic energy, ΔH_f° (298K) was calculated according to the standard convention⁷⁴. Heats of formation of atoms at 0 K, $\Delta H_f^\circ(0\text{ K})$, and enthalpy corrections, for elements in their standard states, $H^\circ(298\text{ K}) - H^\circ(0\text{ K})$ are listed in APPENDIX. Spin-orbit corrections to the electronic energies of atoms, ions, selected diatomic molecules⁷⁵ and acetylene were collected from Refs. 23, 76, and 77.

III. COMPOSITE WAVEFUNCTION THEORIES: G4(MP2) AND CCCA

cWFTs provide molecular thermochemical properties by exploiting the transferability of hierarchical corrections to electronic energies and thermal contributions. In Fig. 1, we present the famous Pople diagram where the desired, albeit expensive, target (non-relativistic) electronic energy at the CCSD(T)/CBS-level can be reached via 3 equivalent additivity routes that is encoded in the G4(MP2) method:

I Reference energy at CCSD(T)/S (small basis) with basis set corrections for electron correlation energy at MP2/S \rightarrow L (small to large basis), and basis set correction for SCF energy HF/L \rightarrow CBS (large to complete basis set).

II Reference energy at MP2/L with post-MP2 correlation with MP2 \rightarrow CCSD(T)/S and basis set correction for SCF energy with HF/L \rightarrow CBS corrections, or

III Reference energy at HF/CBS with electron correlation energy estimated jointly at HF \rightarrow MP2/L and MP2 \rightarrow CCSD(T)/S levels.

The ccCA method differs from G4(MP2) by exactly capturing the MP2-level correlation contribution through a CBS extrapolation of the MP2 energy, and includes post-MP2 level correlation correction with the CCSD(T) method using a triple-zeta basis set. ccCA has separate terms for the relativistic correction and the core-valence effect while G4(MP2) relies on an empirical term – higher level correction (HLC). Both methods account for zero-point vibration energy (ZPVE) by scaling the

harmonic frequencies along with atomic and diatomic spin-orbit (SO) corrections.

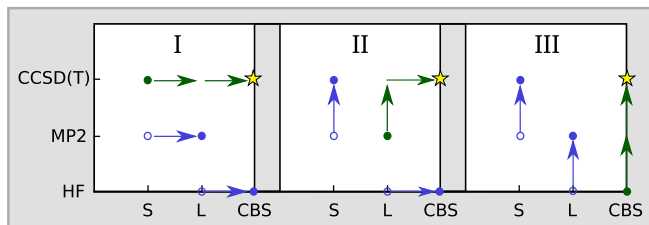


FIG. 1. Three paths to approximate chemical accuracy. Green circle refers to a baseline energy. Green arrows point to exact corrections, while blue arrows correspond to approximate corrections. Blue solid circles imply energy evaluated with a separate calculation while blue open circles imply energy available without an additional calculation. In I, CCSD(T)/S is the starting point while MP2/L, and HF/CBS are the starting points in II and III.

G4(MP2)³⁷ uses a minimum energy geometry at the B3LYP/6-31G(2df,p)-level (basis set henceforth referred to as GTBAS3), followed by a single-point energy calculation at the CCSD(T)/6-31G(d)-level (basis set henceforth referred to as GTBAS1). For molecular enthalpies, vibrational wavenumbers and ZPVEs are calculated using B3LYP/GTBAS3 with harmonic wavenumbers scaled by 0.9854 to approximately account for the missing anharmonic effects⁷⁴. Basis set corrections are included through single point energy corrections at MP2 and HF levels through a focal-point analysis⁷⁸ (see Fig. 1). *Gn*-series closely follows Route-I in Fig. 1, where the expensive $E_{\text{CBS}}^{\text{CCSD(T)}}$ target is estimated as

$$E_{\text{CBS}}^{\text{CCSD(T)}} \approx E_{\text{GTBAS1}}^{\text{CCSD(T)}} + \Delta E^{\text{MP2}} + \Delta E^{\text{HF}} \quad (1)$$

ΔE^{MP2} providing the basis set effect on the correlation energy and ΔE^{HF} aiming to improve the HF energy to the HF-limit:

$$\Delta E^{\text{MP2}} = E_{\text{G3MP2LargeXP}}^{\text{MP2}} - E_{\text{GTBAS1}}^{\text{MP2}} \quad (2)$$

G3MP2LargeXP is a modified form of the 6-311+G(3df,2p) basis set with 3df polarization functions for the first row elements, 4d2f functions for the second row elements and 3d2f functions for the third row elements.

$$\Delta E^{\text{HF}} = E_{\text{CBS}}^{\text{HF}} - E_{\text{G3MP2LargeXP}}^{\text{HF}}, \quad (3)$$

where the HF-limit energy, $E_{\text{CBS}}^{\text{HF}}$, is obtained through a two-point extrapolation of HF/mTZ and HF/mQZ energies:

$$E_{\text{CBS}}^{\text{HF}} = (E_{\text{mQZ}}^{\text{HF}} - e^{-\alpha} E_{\text{mTZ}}^{\text{HF}}) / (1 - e^{-\alpha}) \quad (4)$$

where e is the base of the natural logarithm, and $\alpha = 1.63$. The mXZ basis sets are modifications of the corresponding aug-cc-pVXZ basis sets with an inclusion

of tight d function for the atoms Al-Ar. To reduce the computational cost, the number of diffuse functions on heavy atoms and the size of the hydrogen basis set are trimmed. For detailed descriptions regarding modifications to all the basis sets, please see Refs. 23, 37, 77, and 79.

The total G4(MP2) electronic energy takes the form

$$E_0^{\text{G4(MP2)}} = E_{\text{GTBAS1}}^{\text{CCSD(T)}} + \Delta E^{\text{MP2}} + \Delta E^{\text{HF}} + \text{ZPVE} + \text{SO} + \text{HLC} \quad (5)$$

The HLC term, as pointed out by Martin^{21,80–83}, accounts for the residual error introduced in the additive model when there is significant coupling between the one-particle basis set and N -electron correlated wavefunction. However, it is long known that the success of the HLC correction in G_n methods is strongly coupled to the choice of basis sets employed. To quote John Pople⁸⁴—from the first study on the G1 method—“Uniform application of the HLC is only sensible if the basis used, 6–311+G** (2df), is reasonably balanced, meaning that residual errors per electron are approximately constant over a wide range of molecules.”. HLC has been modified over the years through G1⁸⁴, G2⁸⁵, G3⁷⁹ and G4²³ studies. In G4(MP2)³⁷, the HLC terms take the same form as in G4 but with parameters optimized separately:

$$\text{HLC}^{\text{G4(MP2)}} = \begin{cases} -An_\beta \\ -A'n_\beta - B(n_\alpha - n_\beta) \\ -Cn_\beta - D(n_\alpha - n_\beta) \\ -E \end{cases} \quad (6)$$

where the terms bear the same meaning as in the original G4 study²³.

On the other hand, the ccCA method, developed by Wilson *et al.* is devoid of any such empirical term²⁴. As in the G4(MP2) method, ccCA depends on a reference geometry and harmonic vibrational frequencies computed with B3LYP/GTBAS3. The baseline for ccCA is the MP2-limit energy, $E_{\text{CBS}}^{\text{MP2}}$, with correlation energy corrections, ΔE^{CC} , included at the CCSD(T)/cc-pVTZ level. Of the many ccCA variants developed by Wilson *et al.*^{24,25,38,86–88}, here, we consider ccCA-P²⁵, henceforth referred as ccCA. This method uses a 3-point extrapolation formula to determine $E_{\text{CBS}}^{\text{MP2}}$,

$$E(x) = E_{\text{CBS}} + Be^{-(x-1)} + Ce^{-(x-1)^2}, \quad (7)$$

where $x = 2, 3$ and 4 correspond to MP2/aug-cc-pVXZ ($X = \text{T, D, and Q}$) energies, respectively, and gets simplified to:

$$E_{\text{CBS}}^{\text{MP2}} = (\alpha_1 E_{\text{DZ}}^{\text{MP2}} - \alpha_2 E_{\text{TZ}}^{\text{MP2}} + \alpha_3 E_{\text{QZ}}^{\text{MP2}}) / \beta \quad (8)$$

where, $\alpha_1 = 1 + e^2$, $\alpha_2 = e^1 + e^3 + e^5$, $\alpha_3 = e^6$, and $\beta = (e - 1)(e^5 - e^2 - 1)$. The final working equation for ccCA stands as

$$E_0^{\text{ccCA}} = E_{\text{CBS}}^{\text{MP2}} + \Delta E^{\text{CC}} + \Delta E^{\text{DK}} + \Delta E^{\text{CV}} + \text{ZPVE} + \text{SO} \quad (9)$$

where ΔE^{DK} accounts for scalar relativistic correction calculated using the spin-free, one-electron Douglas-Kroll-Hess Hamiltonian of second-order (DKH2)^{89–92} with frozen-core MP2 energy at cc-pVTZ-DK basis sets, whereas ΔE^{CV} accounts for core-valence correlation effects (see Refs. 24, 25, and 93).

ZPVE & SO are the zero-point vibration energy (computed with a scaling factor of 0.9854⁷⁴) and spin-orbit correction terms, respectively. For the first-row atoms, the MP2 calculation accounts for correlation effects from all electrons, while for the second- and third-row atoms, only those electrons in the K -shell, and $K, \&L$ -shells are kept frozen, respectively. Further, ccCA employs tight- d basis sets—cc-pV($x + d$)Z, aug-cc-pV($x + d$)Z and aug-cc-pCV($x + d$)Z—for second-row elements (Na-Ar) to consider core polarization effects and core-valence basis sets for Ga-Kr developed by Wilson *et al.*^{94,95}.

IV. BENCHMARK DATASET OF MOLECULAR STANDARD FORMATION ENTHALPIES

We have gathered benchmark values of ΔH_f° from six previously studied datasets amounting to 2,271 entries:

1. G3/05 dataset³⁹ is a set of 454 energies distributed into: 270 ΔH_f° , 105 ionization energies (IE), 63 electron affinities (EA), 10 proton affinities (PA), and 6 binding energies (BE) of hydrogen-bonded complexes. This set has been extensively used in the development of the G_n theories and also in the validation of other *ab initio* thermochemical protocols. We have selected all 270 values of ΔH_f° from this set. We note in passing that the original dataset includes 22 atomization energies that we retain.
2. Alexandria dataset⁹⁶ contains classes of molecules similar to that of G3/05 but larger in number with variations in molecular size, thus, providing a platform to examine the transferability of methods that perform well for G3/05. Out of 2704 entries in this dataset, 1392 compounds that contain experimental values of ΔH_f° have been selected.
3. Pedley CHONF is a set of 463 experimental values for hydrocarbons and substituted hydrocarbons from Pedley’s report³⁶ containing the atoms H, C, N, O, and F. An earlier study⁵ has benchmarked the accuracy of G4(MP2) for this dataset and reported an average prediction error of 0.8 kcal/mol.
4. ISO-8 comprises experimental isomerization energies—derived from ΔH_f° —for 8 sets of constitutional isomers amounting to 64 entries⁹⁷.

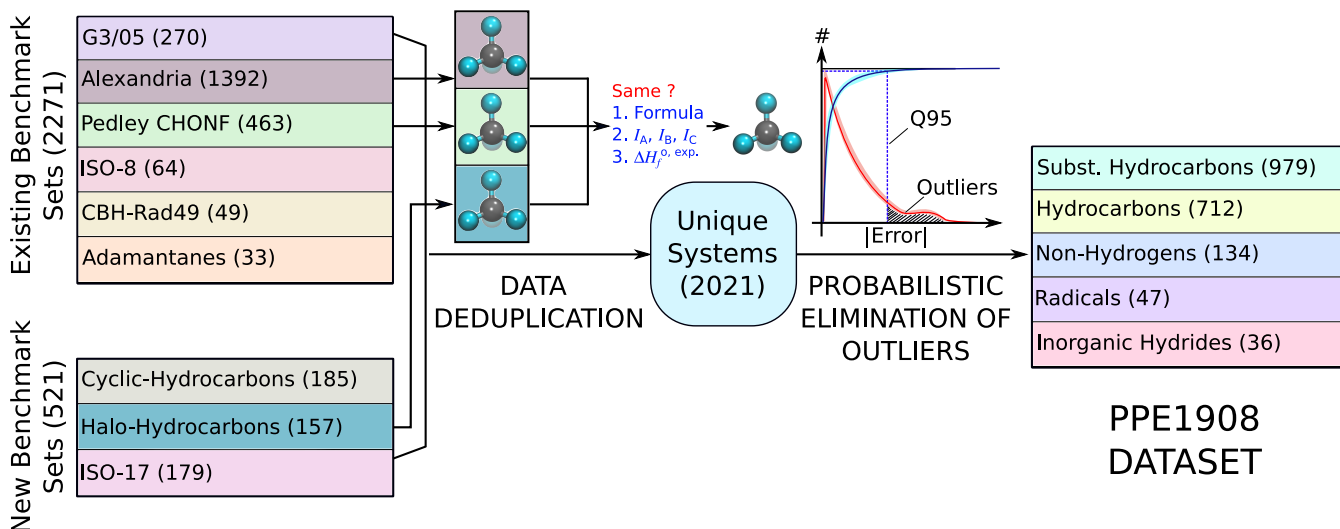


FIG. 2. PPE1908 dataset of molecular standard formation enthalpies: Data collection, deduplication and probabilistic filtering of outliers. See text for more details of the individual datasets and their sources.

5. CBH-rad49⁹⁸ contains a collection of 49 cyclic & acyclic radicals with diverse functional groups and hybridizations. Reference ΔH_f° energies in this dataset are collected from a wide range of resources, combining values from experiments and high-level theoretical modeling.
6. Dorofeeva *et al.*⁹⁹ have presented a dataset of 33 adamantanes for which ΔH_f° were estimated by simultaneous least-squares regression of a thermochemical network containing 300 isodesmic reactions.

Among all the datasets considered here, only G3/05 has been studied with DFT, WFTs and cWFTs^{37–39}, hence, serve as a critical dataset to evaluate the accuracy of thermochemistry methods. To further enrich the benchmark set, we included 521 compounds from Ref. 36 that have never been subjected to theoretical modeling; these compounds belong to the following three categories: cyclic hydrocarbons, halogen-rich hydrocarbons and constitutional isomers with 17 unique stoichiometries. The number of compounds added from each of the aforesaid dataset is shown in Fig. 2. The total number of compounds from the collective set amounts to 2792, where we found a number of repeated entries. To eliminate redundant values, we followed a data deduplication procedure which compares molecular stoichiometries, principal moments of inertia of the geometry and experimental values of ΔH_f° for every pair of molecules. When multiple values of ΔH_f° differing by > 0.1 kcal/mol were found for the same compound, we have retained the more frequently studied entry.

For the resulting dataset of 2021 compounds, it is a non-trivial task to quantify—*ab initio*—plausible uncer-

tainties arising not only from random and systematic errors in the experimental measurements, but also due to ambiguities associated with the empirical parameters used in the estimation of ΔH_f° . Paulechka *et al.*¹⁰⁰ have discussed the reasons for typical uncertainties in experimentally determined ΔH_f° and indicated that these could be of the order of even a few kJ/mol. In that study, for very critical benchmarking of the DLPNO-CCSD(T) based estimation of ΔH_f° , the authors have selected 45 compounds for which at least two independent experimental results were available. Even when using such ‘precise’ experimental values as references, error trends based on the mean unsigned error (MUE) can severely underestimate thermochemical uncertainty¹⁰¹. Simm *et al.*¹⁰² have discussed how a performance analysis based on MUE is prone to fail as it does not distinguish the systematic contributions to the errors from the non-systematic counterparts. For pathological error distributions, arising plausibly due to the presence of outliers in the reference dataset, prediction uncertainties can be truncated using percentile-based error metrics^{101,103–105}. More specifically, performance ranking of *ab initio* methods revealing trends in uncertainties has been made possible by the use of the 95th percentile of the absolute intensive (*i.e.* normalized) error distributions along with the MUE¹⁰⁶. It is the subject of Section V to discuss a procedure to detect probabilistic tendencies of a reference datum from the 2021 set to be an outlier.

V. PROBABILISTIC PRUNING OF THE DATASET

Following the data deduplication step, we utilize a probabilistic argument to detect outliers in the resulting dataset with 2021 entries. The basic principle behind

this scheme is to utilize highly accurate computed values of ΔH_f° as references and mark only those molecules that lie beyond the 95th percentile of the error distribution as outliers. The cumulative probability used for this purpose acts as a prior distribution—more robust the reference method, more reliable the prior probability is. Hence, it may be anticipated that this scheme is guaranteed to detect genuine outliers when one of the high-precision methods such as W4, HEAT-456QP, or HEAT-345QP is used as a reference. Given the size of majority of the molecules in the dataset, we depend on G4(MP2) predicted values to define the prior probability; computational details of the calculations are deferred to Section III.

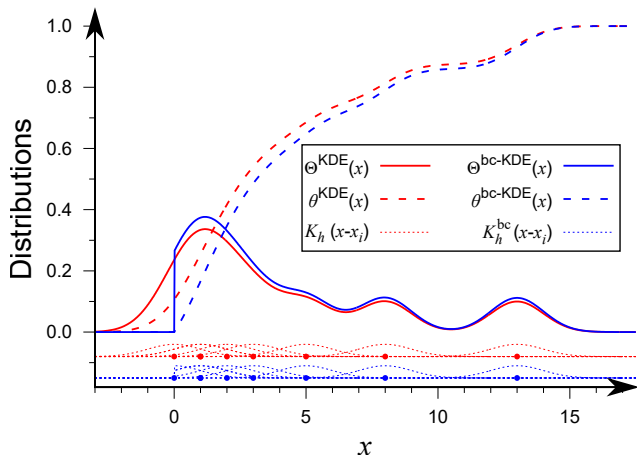


FIG. 3. Probability density function, $\theta(x)$, and cumulative distribution function, $\Theta(x)$, based on kernel density estimation (KDE) and its boundary corrected analog, bc-KDE, demonstrated for an exemplary dataset with eight points: $x_1 = 0$, $x_2 = x_3 = 1$, $x_4 = 2$, $x_5 = 3$, $x_6 = 5$, $x_7 = 8$ and $x_8 = 13$. For clarity, $\theta(x)$ has been multiplied by 100. Also shown in the bottom of the plot are the kernel basis functions $K_h(x - x_i)$ and $K_h^{\text{bc}}(x - x_i)$ centered at the data points with arbitrarily shifted ordinates.

We begin with the absolute errors in the G4(MP2) predicted ΔH_f° for the 2021 set. We followed the arguments presented by Savin *et al.*¹⁰⁷ and Perdew *et al.*¹⁰⁸, and chose an intensive error measure in order to account for the fact that the dataset contains molecules covering various sizes. For this purpose, we used MUE per valence electron, to capture periodic trends in molecular thermochemistry. From the discrete values of the G4(MP2) error, we obtain a continuous probability distribution using the boundary corrected kernel density estimation (bc-KDE), where a radial basis function is expanded at each discrete value of the error. In KDE, we take a kernel in the form of the standard normal distribution $\mathcal{N}(0, 1)$

$$K_h(x - x_i) = \frac{1}{\sqrt{2\pi}h} \exp\left[-\frac{(x - x_i)^2}{2h^2}\right], \quad (10)$$

where K_h is the normalized estimator. A kernel function is expanded at every data point, giving rise to the (un-normalized) total density function that is an average of all kernels

$$\hat{f}(x, h) = \frac{1}{N} \sum_{i=1}^N K_h(x - x_i) \quad (11)$$

It is a well-known problem that KDE can delocalize beyond the allowed domain; in such cases, the naive approach of truncating the total density function $f(x)$ often underestimates the actual probability distribution. This effect is illustrated using a toy dataset in Fig. 3. To this end, we employ boundary-corrected kernels of the form

$$K_h^{\text{bc}}(x - x_i) = [K_h(x - x_i) + K_h(x + x_i - 2x^*)] \mathbf{1}_{x \in A}, \quad (12)$$

where the indicator function $\mathbf{1}_{x \in A}$ is 1 when $x \in A$ and vanishes otherwise¹⁰⁹. As is evident from Fig. 3, the bc-KDE captures the true nature of the probability density when the property is bounded. While the individual kernel functions that cross the boundary are truncated by the indicator function, the total probability is still conserved through a normalization of the resulting probability density, see Eq. 14.

In our bc-KDE calculations, we used a kernel width of 0.005 kcal/mol and determined the total density function as the average

$$\hat{f}(x, h) = \frac{1}{N} \sum_{i=1}^N [K_h(x - x_i) + K_h(x + x_i - 2x^*)] \mathbf{1}_{x \in A}, \quad (13)$$

which is normalized over the domain to give the probability density function (PDF)

$$\hat{\phi}(x) = \frac{\hat{f}(x, h)}{\|\hat{f}(x, h)\|_2}. \quad (14)$$

The cumulative density function (CDF) used to identify percentiles is obtained by integrating the PDF

$$\hat{\Phi}(x) = \int_A^B dx \hat{\phi}(x). \quad (15)$$

The resulting CDF enables statistical modeling of the probability to obtain a certain degree of prediction accuracy for a given quantum chemistry method as previously noted by Pernot *et al.*¹⁰³. To estimate the variance of the CDF, we followed bootstrapping with 1000 shuffles, with 500 points randomly sampled from the 2021 set. The boundary-corrected kernel density probability distribution, $\theta^{\text{bc-KDE}}$ and the corresponding cumulative density function $\Theta^{\text{bc-KDE}}$ are on display in Fig. 4. To eliminate any sampling bias, we use the lower bound of the 95th percentile, denoted $Q95^-$ in Fig. 4 as

a threshold; all compounds for which the MUE per valence electron is greater than Q_{95^-} are marked as outliers and eliminated from the dataset. We thus arrive at the benchmark set of probabilistically pruned enthalpies of 1908 compounds, denoted henceforth PPE1908. In this way, elimination of 113 outliers from the original 2021 set, decreased G4(MP2)'s MUE for the dataset from 2.10 kcal/mol to 1.65 kcal/mol. This final MUE is 0.66 kcal/mol larger than the methods MUE for the G3/05 dataset with 270 values of ΔH_f° . In SectionVID, we discuss how the performance of cWFTs and DFAs deteriorate systematically because of the uncertainties associated with empirical atomic parameters used in the calculation of thermochemistry energetics. Compared to the small molecules benchmark set G3/05, PPE1908 covers the space of molecules that contain more atoms as well as more valence electrons; qualitative trends are illustrated in Fig. 5. The largest number of valence electrons in G3/05 and PPE1908 sets are 66 (C_6F_6 and C_6F_5Cl) and 166 ($C_{10}F_{18}$), respectively. On the other hand, the maximum number of atoms in a given compound is 26 (C_8H_{18}) for the G3/05 set, and 56 ($C_{18}H_{37}Cl$) for PPE1908. Both sets are dominated by closed-shell molecules as evident from larger counts for compounds with even number of valence electrons, see Fig. 5a.

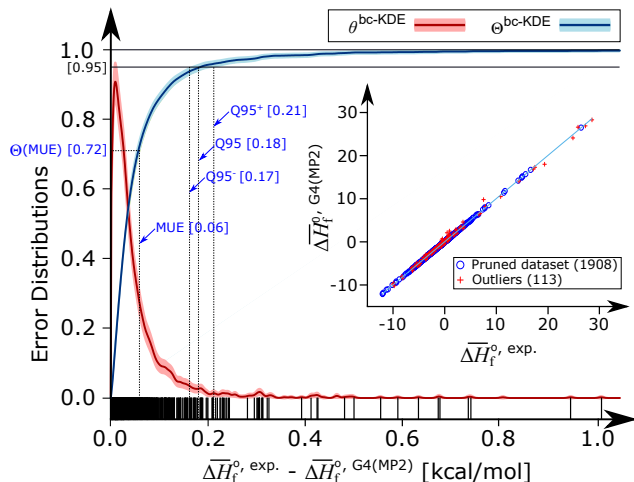


FIG. 4. Boundary-corrected kernel density probability distribution, ρ^{bc-KDE} and the corresponding cumulative density function Θ^{bc-KDE} for the absolute deviations of G4(MP2)-predicted ΔH_f° from the experimental ones for 2021 compounds. The overline indicates that the values are normalized over valence electrons. Uncertainty envelopes were determined by bootstrapping. The inset features a scatterplot.

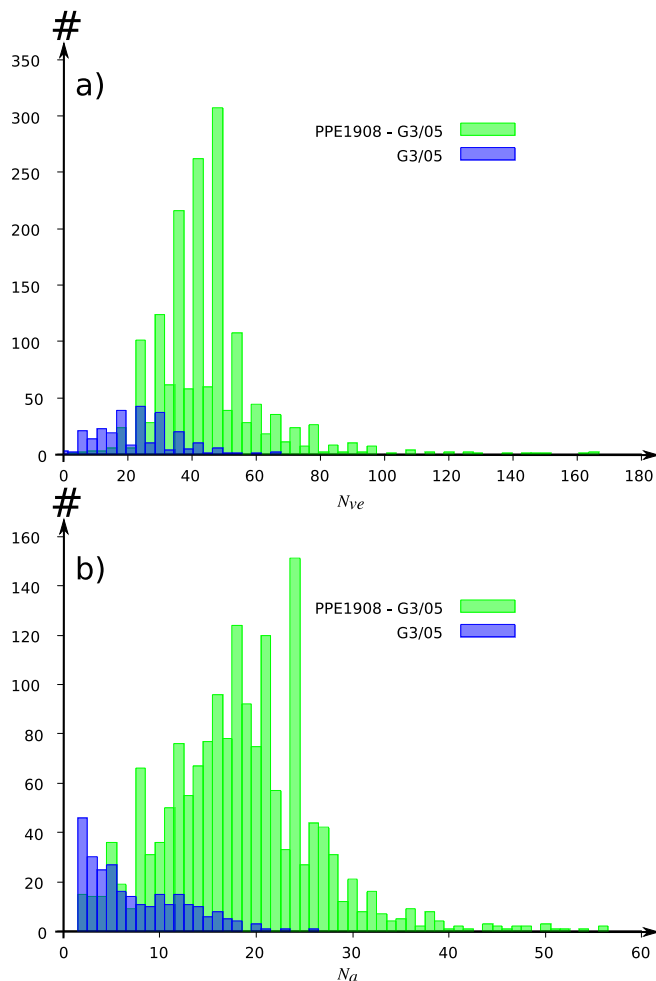


FIG. 5. Distribution of compounds in the G3/05 dataset compared to other molecules that are present in PPE1908: a) Counts for number of valence electrons N_{ve} , b) Counts for number of atoms N_a .

VI. RESULTS AND DISCUSSIONS

A. Benchmark results for cWFTs and DFAs

While cWFTs are the recommended choice for modeling ΔH_f° , the favorable accuracy-to-speed trade-offs of DFAs have facilitated ΔH_f° predictions for large molecules through isodesmic reaction schemes^{110,111} and group additivity schemes¹¹². A benchmark across popular DFAs on a curated dataset such as PPE1908 (see Fig. 5), may provide insights into how the performances of these methods can be refined through proper selection of basis sets and additional dispersion corrections. To this end, we embark upon comprehensive benchmarking of G4(MP2), ccCA, 23 popular DFAs as well as the semi-empirical methods, PM6 and PM7.

Table I summarizes MUEs, RMSEs and maximum errors for each method across various classes of compounds in PPE1908. It is apparent while moving

TABLE I. Prediction errors in the modeling of ΔH_f° . For selected cWFTs, DFAs and semi-empirical methods, mean unsigned error (MUE) is reported for each class of compounds in the PPE1908 benchmark dataset. The root-mean-square-error is given in parenthesis while, the most positive and negative errors are provided inside a square bracket. All values are in kcal/mol.

Methods	Nonhydrogens (134)	Hydrocarbons (712)	Subst. hydrocarbons (979)	Inorganic hydrides (36)	Radicals (47)	Total (1908)
G4 (MP2)	1.73 (2.50) [-8.10, 7.63]	1.76 (2.68) [-10.47, 18.08]	1.59 (2.23) [-10.70, 11.15]	0.91 (1.30) [-4.15, 1.96]	1.38 (1.95) [-6.14, 5.31]	1.65 (2.41) [-10.70, 18.08]
ccCA ^a	1.72 (2.59) [-10.56, 6.06]	1.79 (2.51) [-9.60, 19.71]	1.61 (2.28) [-9.81, 10.50]	1.08 (1.37) [-3.19, 2.99]	1.65 (2.57) [-10.35, 1.57]	1.67 (2.38) [-10.56, 19.71]
PM6	16.49 (36.65) [-40.57, 173.87]	3.73 (5.20) [-11.99, 42.14]	3.57 (12.45) [-25.88, 363.85]	23.51 (61.83) [-9.07, 253.15]	15.13 (22.03) [-41.88, 97.57]	5.20 (16.37) [-41.88, 363.85]
PM7	17.96 (35.27) [-72.66, 151.64]	3.37 (4.50) [-16.95, 23.05]	3.26 (12.39) [-28.91, 365.66]	23.81 (62.35) [-14.44, 245.37]	13.73 (21.57) [-42.78, 105.04]	4.98 (16.08) [-72.66, 365.66]
BLYP	11.50 (15.75) [-51.31, 52.50]	38.88 (43.23) [-149.31, 6.68]	20.35 (25.42) [-146.46, 44.73]	7.13 (10.23) [-22.54, 30.66]	13.59 (20.43) [-64.24, 26.33]	26.23 (32.54) [-149.31, 52.50]
PW91	23.14 (31.18) [-29.53, 94.31]	42.70 (48.77) [-0.00, 208.96]	41.39 (47.08) [-5.23, 170.02]	8.35 (14.40) [-7.05, 49.25]	22.55 (27.29) [-3.12, 62.29]	39.51 (46.00) [-29.53, 208.96]
PBE	22.40 (30.38) [-28.47, 91.58]	37.90 (44.62) [-0.21, 203.43]	37.80 (43.78) [-5.58, 160.27]	8.94 (14.43) [-10.63, 49.36]	20.87 (25.44) [-2.05, 62.86]	35.80 (42.56) [-28.47, 203.43]
TPSS	5.93 (8.44) [-17.62, 35.52]	4.53 (5.60) [-32.48, 14.14]	4.78 (6.25) [-33.82, 30.10]	5.51 (7.19) [-13.18, 18.41]	6.28 (7.00) [-8.28, 12.68]	4.82 (6.24) [-33.82, 35.52]
B3LYP	9.91 (13.43) [-44.02, 7.77]	20.26 (23.26) [-90.90, 1.22]	14.00 (17.36) [-93.18, 4.88]	4.15 (6.20) [-19.02, 11.40]	6.81 (11.08) [-37.63, 6.04]	15.69 (19.31) [-93.18, 11.40]
B3LYP-D3	5.93 (7.55) [-22.89, 10.71]	3.74 (4.71) [-15.05, 25.03]	4.20 (6.09) [-41.04, 17.68]	3.78 (5.14) [-13.47, 13.17]	3.86 (4.57) [-10.33, 10.18]	4.13 (5.69) [-41.04, 25.03]
O3LYP	24.37 (33.28) [-21.61, 109.13]	95.53 (100.94) [-0.00, 290.86]	74.49 (80.89) [-15.12, 225.98]	12.08 (16.11) [-10.06, 46.76]	39.32 (50.23) [-8.40, 110.02]	76.78 (85.46) [-21.61, 290.86]
X3LYP	9.57 (12.85) [-42.18, 8.10]	19.54 (22.27) [-85.66, 0.62]	13.74 (16.73) [-88.04, 3.91]	4.15 (6.16) [-19.95, 9.18]	6.45 (10.62) [-35.65, 5.36]	15.25 (18.54) [-88.04, 9.18]
PBE0	5.21 (7.21) [-18.56, 27.76]	12.15 (16.90) [-2.55, 88.73]	8.41 (11.80) [-16.21, 46.92]	5.59 (6.59) [-16.37, 8.19]	6.20 (9.04) [-2.75, 33.17]	9.47 (13.58) [-18.56, 88.73]
TPSS0	15.52 (18.91) [-53.65, 13.80]	7.33 (11.23) [-69.95, 7.09]	14.90 (20.30) [-125.62, 10.27]	9.21 (12.19) [-38.63, 18.55]	6.35 (7.82) [-17.41, 8.38]	11.80 (16.97) [-125.62, 18.55]
TPSS0-D3	12.27 (15.35) [-47.07, 13.20]	10.86 (12.14) [-18.30, 37.22]	9.40 (13.82) [-99.14, 38.28]	9.15 (11.85) [-34.45, 22.95]	7.57 (9.05) [-16.12, 20.44]	10.10 (13.20) [-99.14, 38.28]
M06-2X	4.24 (5.65) [-17.58, 17.87]	6.63 (7.62) [-26.66, 5.36]	3.87 (5.11) [-22.13, 26.54]	3.42 (4.34) [-9.23, 9.32]	3.31 (4.77) [-14.63, 6.08]	4.90 (6.18) [-26.66, 26.54]
M06-2X-D3	4.24 (5.66) [-17.58, 17.87]	6.21 (7.12) [-23.80, 5.47]	3.70 (4.94) [-22.12, 27.65]	3.42 (4.34) [-9.23, 9.32]	3.23 (4.67) [-14.44, 6.08]	4.66 (5.88) [-23.80, 27.65]
ω B97X	3.51 (4.45) [-15.54, 11.55]	3.58 (4.43) [-21.78, 8.70]	2.57 (3.57) [-19.45, 13.03]	2.87 (3.56) [-8.30, 6.35]	2.34 (3.32) [-9.50, 7.48]	3.01 (3.97) [-21.78, 13.03]
ω B97X-D3	3.43 (4.39) [-15.68, 8.79]	3.38 (4.09) [-18.75, 8.78]	2.49 (3.46) [-18.74, 11.73]	2.95 (3.71) [-7.37, 6.41]	2.26 (3.22) [-9.50, 7.27]	2.89 (3.78) [-18.75, 11.73]
ω B97X-V	3.30 (4.55) [-10.27, 17.21]	2.39 (3.22) [-15.74, 15.32]	3.12 (4.50) [-12.28, 34.23]	3.16 (3.93) [-7.29, 9.93]	3.04 (3.76) [-7.00, 10.20]	2.86 (4.05) [-15.74, 34.23]
ω B97X-D3Bj	3.92 (5.92) [-13.22, 29.03]	3.62 (4.27) [-18.15, 8.38]	2.58 (3.38) [-17.09, 11.04]	3.91 (4.89) [-7.75, 15.07]	2.36 (3.30) [-8.71, 6.52]	3.08 (3.98) [-18.15, 29.03]
ω B97M-V ^b	5.38 (7.03) [-7.94, 21.77]	15.35 (16.57) [-1.21, 55.99]	12.42 (13.86) [-13.00, 46.15]	3.56 (4.44) [-6.37, 10.78]	6.60 (8.41) [-6.59, 21.09]	12.77 (14.42) [-13.00, 55.99]
ω B97M-D3Bj ^b	3.41 (4.41) [-10.67, 17.12]	8.97 (9.66) [-1.36, 34.11]	6.50 (7.61) [-20.41, 23.61]	3.11 (3.78) [-5.39, 10.05]	4.07 (5.11) [-9.78, 12.10]	7.11 (8.20) [-20.41, 34.11]
CAM-B3LYP	6.88 (9.56) [-36.71, 12.98]	3.79 (5.68) [-30.75, 5.52]	4.00 (5.80) [-31.68, 14.17]	3.28 (4.24) [-12.86, 7.13]	3.89 (4.62) [-11.96, 6.87]	4.11 (6.05) [-36.71, 14.17]
B2PLYP	4.32 (5.65) [-20.23, 10.52]	7.42 (9.19) [-39.19, 12.71]	5.20 (6.72) [-35.64, 11.03]	2.72 (3.66) [-9.29, 10.69]	3.38 (5.08) [-16.51, 5.91]	5.88 (7.61) [-39.19, 12.71]
B2PLYP-D3	3.00 (3.90) [-13.25, 12.24]	4.13 (6.83) [-11.53, 46.82]	3.84 (5.41) [-14.77, 23.40]	2.39 (3.24) [-6.77, 11.46]	2.25 (2.96) [-8.10, 9.29]	3.82 (5.83) [-14.77, 46.82]
mPW2PLYP-D	4.13 (5.26) [-18.03, 5.29]	3.86 (5.10) [-6.42, 30.59]	3.21 (4.23) [-19.63, 15.02]	2.76 (3.53) [-11.42, 6.80]	2.09 (2.80) [-7.74, 6.76]	3.48 (4.61) [-19.63, 30.59]

^a Hydrocarbons: 638, Subst. hydrocarbons: 929, Total: 1784

^b Nonhydrogens: 121, Inorganic hydrides: 33, Total: 1892

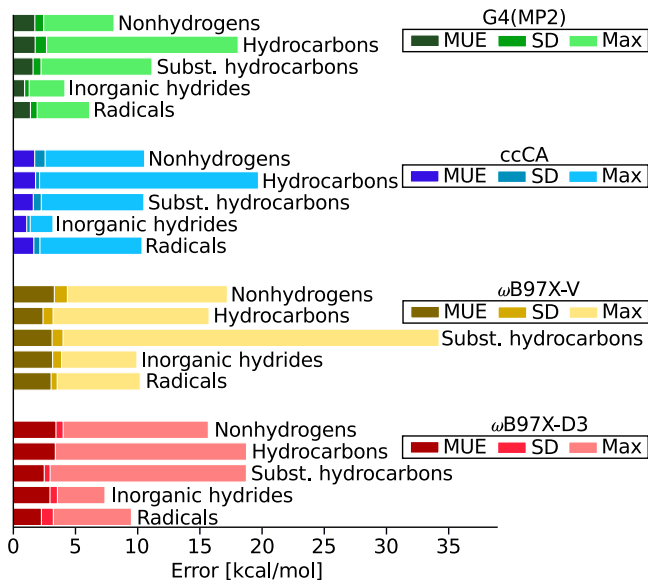


FIG. 6. Prediction errors in ΔH_f^0 across compound types and methods; MUE: mean unsigned error, SD: standard deviation, Max: maximum absolute deviation. For number of entries in each class of compounds and methods, see Table. I

across various subsets, that the performance of cWFTs – G4(MP2) and ccCA – are consistent irrespective of the compound type, with MUEs below 2 kcal/mol. Though somewhat larger error is noted for ccCA modeling of radicals, when compared to the predictions of G4(MP2), the overall deviations arise clearly from the residual selection bias in probabilistic pruning. We note the GGA functionals consistently under-performing across all subsets. A closer look reveals errors to be mostly systematic as higher MUEs are usually encountered for subsets with greater structural complexities. Hybrid GGAs mostly improve upon GGA results (barring O3LYP), by accounting for better approximations of the dispersion interactions. Overall, as we move up the *Jacob’s ladder*⁴⁶, we observe a consistent drop in MUE. Most notably, we find the long-range tuned hybrid DFAs to perform better than double hybrids DFAs. The importance of capturing long-range effects can be further understood by noting that explicit inclusion of an empirical dispersion correction mostly improves the performance across DFAs. Semi-empirical methods PM6 and PM7 under-perform across all subsets except in the case of hydrocarbons, where their accuracy is on par with long-range tuned functionals with PM7 slightly outperforming PM6. For the four best performing methods: G4(MP2), ccCA, ω B97X-D3, and ω B97X-V, we have graphically summarized the error metrics in Fig. 6. As noted before in Table. I, G4(MP2) and ccCA exhibit comparable prediction accuracies. In terms of the maximum absolute deviation (Max), ccCA seems slightly better than G4(MP2) for inorganic hy-

drides. Amongst the DFAs, ω B97X-D3 shows reduced Max than ω B97X-V consistently; the latter has yielded the largest Max values for substituted hydrocarbons, which we believe to stem from the lack of such compounds in the training of that DFA.

A drawback of relying on mean-based error metrics is that, these do not provide a complete picture of the error distribution. For this purpose, percentile-based metrics have been shown to be more suitable (see Ref. 103 and references therein). Fig. 7 presents mean- and percentile-based metrics for all the computational methods studied here. A method with good prediction accuracy should show smaller MUEs as well as small values of Q_N , where $N > 50$. Spearman rank correlation (ρ) between two sets is a good indicator for qualitative agreement between them¹¹³. Compared to 1908 experimental ΔH_f^0 values, we find G4(MP2) and ccCA to show a strong correlation amounting to $\rho = 0.999$. For the DFA, we find dispersion corrections to mostly improve ρ . As noted for MUE, the percentile metrics and the ρ of the semi-empirical methods PM6 and PM7 are consistently superior than that of the GGA methods. This is because these simple methods have been trained to deliver accurate values of ΔH_f^0 for hydrocarbons that also dominate the PPE1908 dataset.

The apparent success of dispersion corrected DFAs motivated us to have a closer look at the effect basis set size has on accuracy. To this end, we have collected ΔH_f^0 values for the 463 systems in the Pedley CHONF dataset (see Section IV) and studied these with def2-XVP (X=S, TZ, and QZ) basis sets using B3LYP and ω B97X DFAs—with and without a D3 term (see Table II). Among all possibilities, we note the performance to be the best for ω B97X-D3 with a QZ basis set. This result is in accord with the findings reported in Ref. 5. Fortuitously, B3LYP achieves minimum error for the smallest basis set, indicating an inconsistent trend in accuracy with basis set size—a trend also noted in Ref. 39. However, we find the D3-corrected B3LYP to somewhat improve this situation. When going from B3LYP to B3LYP-D3, we note a larger gain in accuracy with the QZ basis set; however, for the ω B97X DFA, D3 term only leads to a modest improvement so long as the basis set is QZ.

Examining the compounds showing extreme (*i.e.* most-positive or most-negative) errors for a given computational method often reveals if the error is systematic or non-systematic in nature. For the latter to be evident one has to consider normalized or intensive errors such as error-per-electron or error-per-atom. In the case of G4(MP2), along with the total error, we also consider error-per-valence-electron and inspected those compounds exhibiting extreme errors (see Fig. 8). Barring the hydrocarbons category, we find the compounds with extreme intensive and extensive (*i.e.* unnormalized) error to mostly comprise heavy atoms. Predominant of the compounds with large intensive error are with fewer heavy atoms, while

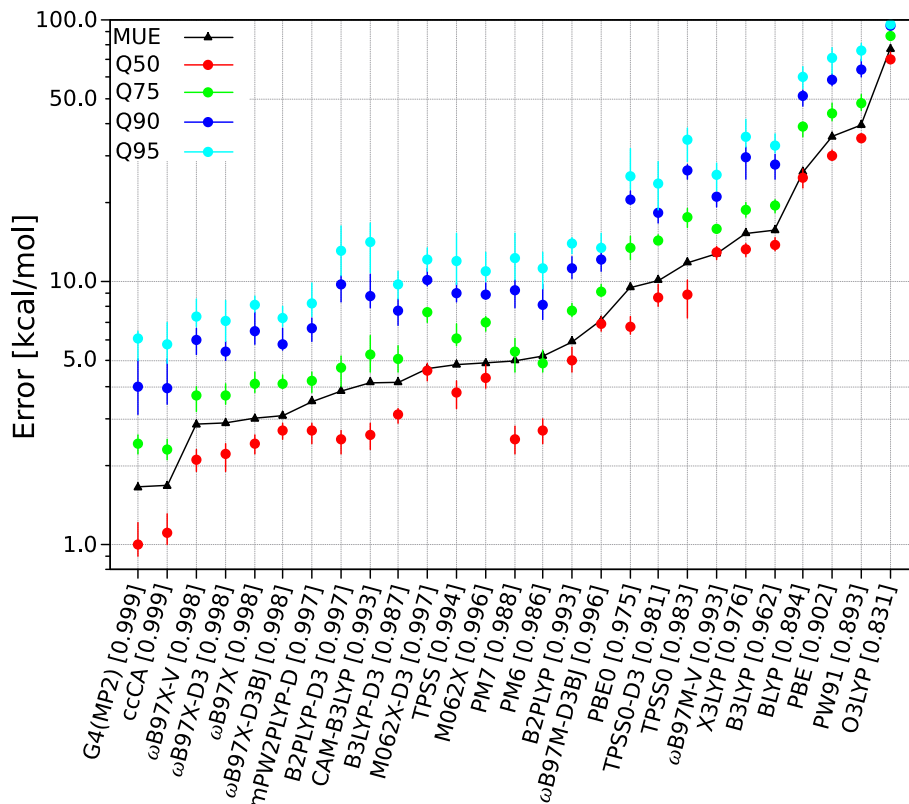


FIG. 7. Ranking of the prediction accuracy of cWFTs, DFAs and semi-empirical models. For each method, the mean unsigned error (MUE) and cumulative probability percentiles, Q_n ($n = 50, 75, 90$, and 95) are reported in log-scale. Methods are sorted in ascending order of MUE. Values in square brackets are the Spearman rank correlations w.r.t experimental values. Vertical lines on the percentile points denote the standard deviation estimated via bootstrapping.

TABLE II. Dependence of prediction accuracy of B3LYP and ω B97X DFAs on the D3 empirical dispersion correction and def2-XVP ($X = S/TZ/QZ$) basis sets. For a given DFA and basis set, MUE in the predicted ΔH_f° is reported when compared to experimental values. The benchmark dataset comprises 463 molecules (“Pedley CHONF dataset”) with 178 hydrocarbons and 285 substituted hydrocarbons. All values are reported in kcal/mol.

Dataset	B3LYP			B3LYP-D3			ω B97X			ω B97X-D3		
	S	TZ	QZ	S	TZ	QZ	S	TZ	QZ	S	TZ	QZ
Hydrocarbons (178)	2.64	16.52	13.79	15.53	1.80	2.91	12.74	4.23	2.23	12.80	4.45	2.17
Subs. hydrocarbons (285)	5.04	11.72	9.24	16.05	2.84	3.78	11.95	3.49	1.75	11.97	3.57	1.72
Total (463)	4.14	13.57	10.99	15.85	2.44	3.44	12.25	3.78	1.93	12.29	3.91	1.89

those with large extensive (or unnormalized) error consist of either a large number of atoms or contain several heavy atoms. Hydrocarbons cycloheptadecane and 9,10-diphenylanthracene feature the largest extensive error; from opposite signs of the errors of these two compounds, one may speculate that the source of their errors cannot be due to the uncertainties associated with the parameters used in the enthalpy evaluation (see Section VID for a discussion). Interestingly, the radical 1-norbornyl features on both columns of Fig. 8, plausibly owing to less diversity in this class. A specialized study on these extreme compounds displayed in Fig. 8 with more robust cWFTs or WFTs should reveal further insights into both, the deficiencies of G4(MP2) in modeling the ΔH_f° of these systems, and also clarify the uncer-

tainties in the experimental results.

It is important to compare the accuracy of the G4(MP2) and ccCA results presented above, based on the present implementation, to that of legacy implementations of these cWFTs. Firstly, all our calculations are based on a framework employing spherical primitive Gaussian type orbitals (GTOs), while Pople basis sets—used for B3LYP geometry relaxation, and G4(MP2) energies—are conventionally used in the Cartesian primitive GTO framework. Secondly, the ccCA-P³⁸ formalism uses B3LYP/cc-pVTZ reference geometry with Hartree-Fock and MP2 energies extrapolated separately to the CBS limit, relativistic DKH2 corrections for open-shell molecules calculated with a spin-collinear (*i.e.* UHF) reference wavefunction, and em-

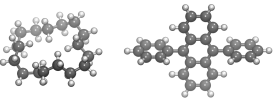
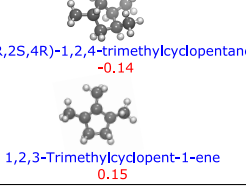
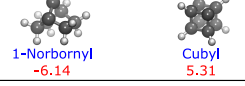
	Error	Error per valence electron
Nonhydrogens	 Octafluoropropane -8.10 Hexachloroethane 7.63	 Gallium fluoride -0.16 Carbonyl sulfide 0.16
Hydrocarbons	 Cycloheptadecane -10.47 9,10-Diphenylanthracene 18.08	 (1R,2S,4R)-1,2,4-trimethylcyclopentane -0.14 1,2,3-Trimethylcyclopent-1-ene 0.15
Subst. Hydrocarbons	 1,2-Dibromo-1-chloro-1,2,2-trifluoroethane -10.70 1-Bromo-pentafluorobenzene 11.15	 3-Fluoro-propene -0.17 Tetrachloroethylene 0.17
Inorganic hydrides	 Dihydrogen sulfate -4.15 Disilane 1.96	 Difluorosilane -0.17 Silane 0.16
Radicals	 1-Norbornyl -6.14 Cubyl 5.31	 1-Norbornyl -0.16 Phosphinyl 0.16

FIG. 8. Left column presents molecules in the PPE1908 dataset exhibiting the highest deviations in G4(MP2) predicted ΔH_f° . Right column shows molecules with extreme errors per valence electron.

employs a different scale factor for ZPVE. To this end, in Table III, we compare prediction errors in our cWFT calculations for the entire G3/05 dataset to that of previously published results with same methods. For comparison, we have also summarized previous results based on the more accurate G4 theory.

As far as the G4(MP2) results are concerned, going from Cartesian GTOs to spherical GTOs leads to a tiny increase in the MUE by 0.01 kcal/mol. When inspecting the individual results for various class of compounds and properties, we note the error to be largest for the electron affinity (EA) of atoms, where the rise in error is 0.04 kcal/mol. This is expected, as the energy of atomic anions should suffer the maximum loss in the basis function count per electron. Our prediction error for ccCA fares rather well when compared to ccCA-P values from Ref. 38, while the original formalism—with a larger basis set for geometry optimization—showing much smaller error for the binding energy of hydrogen bonded dimers. We believe that the accuracy of our ccCA results can improve when adopting the ccCA settings to be similar to that of the ccCA-P³⁸ implementation, however, here we have used settings that will render the comparison between G4(MP2) and ccCA seamless.

Further, we have extended the comparison between cWFTs to the slightly larger dataset – Pedley CHONF

TABLE III. Comparison between errors in G4(MP2), ccCA and G4 for G3/05 and Pedley CHONF. Both results from previous and current studies are included for all classes of compounds.

Dataset	G4(MP2)	ccCA	G4
I. G3/05 (452) ^a	1.05, 1.04 ^b	0.98, 0.99 ^c	0.83 ^d
1. ΔH_f° (270)	0.99, 0.99 ^b	0.92, 0.95 ^c	0.80 ^d
-Nonhydrogens (79)	1.44, 1.44 ^b	1.05	1.13 ^d
-Hydrocarbons (38)	0.64, 0.63 ^b	0.95	0.48 ^d
-Subst. Hydrocarbons (100)	0.84, 0.83 ^b	0.85	0.68 ^d
-Inorganic hydrides (19)	0.92, 0.94 ^b	0.99	0.92 ^d
-Radicals (34)	0.85, 0.86 ^b	0.78	0.66 ^d
2. IP (103) ^a	1.08, 1.07 ^b	1.08, 1.09 ^c	0.91 ^d
-Atoms (26)	1.12, 1.13 ^b	0.55	0.65 ^d
-Molecules (77)	1.06, 1.05 ^b	1.26	0.99 ^d
3. EA (63)	1.26, 1.23 ^b	0.97, 1.03 ^c	0.83 ^d
-Atoms (14)	1.86, 1.84 ^b	0.89	0.91 ^d
-Molecules (49)	1.10, 1.06 ^b	1.00	0.81 ^d
4. PA (10)	0.66, 0.67 ^b	1.17, 0.93 ^c	0.84 ^d
5. BE (6)	1.29, 1.28 ^b	1.15, 0.58 ^c	1.12 ^d
II. Pedley, ΔH_f° (463)	0.78, 0.79 ^e	1.02	
-Hydrocarbons (178)	0.62, 0.68 ^e	0.90	
-Subst. hydrocarbons (285)	0.88, 0.86 ^e	1.09	

^a We have excluded two triplet entries for H₂S and N₂

^b from Ref. 37

^c from Ref. 38

^d from Ref. 23

^e from Ref. 5

(see SectionIV); we note our G4(MP2) results to agree fairly well with that of previously reported values from Ref. 5. Interestingly, for G4(MP2) we find the accuracies for hydrocarbons and their substituted analogues to be retained when going from the G3/05 set to Pedley CHONF. As for ccCA, the MUE of 1.02 kcal/mol for the Pedley CHONF dataset is comparable to that of the total error for the G3/05 set, indicating the small deviations in both values to lie within the uncertainties in the reference experimental values.

B. Role of HLC in G4(MP2) and its Transferability across Datasets

An interesting point of concern in the G_n -series of cWFTs—more specifically G4(MP2)—is the role HLC plays in the model (see Eq. 5). To gain more insight on this point, we present the error in G4(MP2) predictions with successive inclusion of energy terms in Fig. 9 for the case of 270 ΔH_f° values from the G3/05 set. The distributions are shown for both extensive and intensive errors. In both cases, the CCSD(T) error distribution is broad and multimodal, narrowing with successive inclusion of $\Delta MP2$ and ΔHF corrections. The error in the resulting model exhibits a spread: -50 kcal/mol to 10 kcal/mol for the extensive errors, which is quenched by the inclusion of the HLC term. It is remarkable that the HLC term, given its simple form, not only shifts

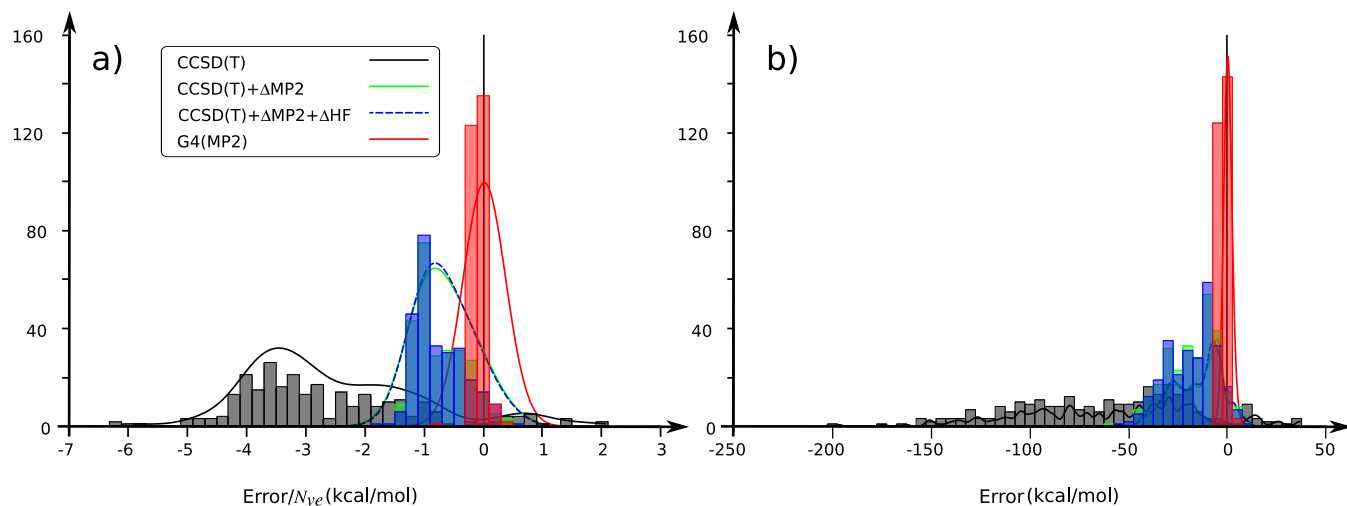


FIG. 9. Effect of systematic inclusion of components in the G4(MP2) ΔH_f° on error distribution; SO, ZPVE and thermal corrections have been included in all calculations. For 270 molecules from the G3/05 dataset, error distribution of predicted ΔH_f° are shown: a) per valence electron (*i.e.* Error/ N_{ve}), and b) without normalization. Black boxes stand for CCSD(T) values, green ones correspond to values with Δ MP2 corrections, blue correspond to results with further inclusion of Δ HF corrections, and the final G4(MP2) results with HLC are shown in red.

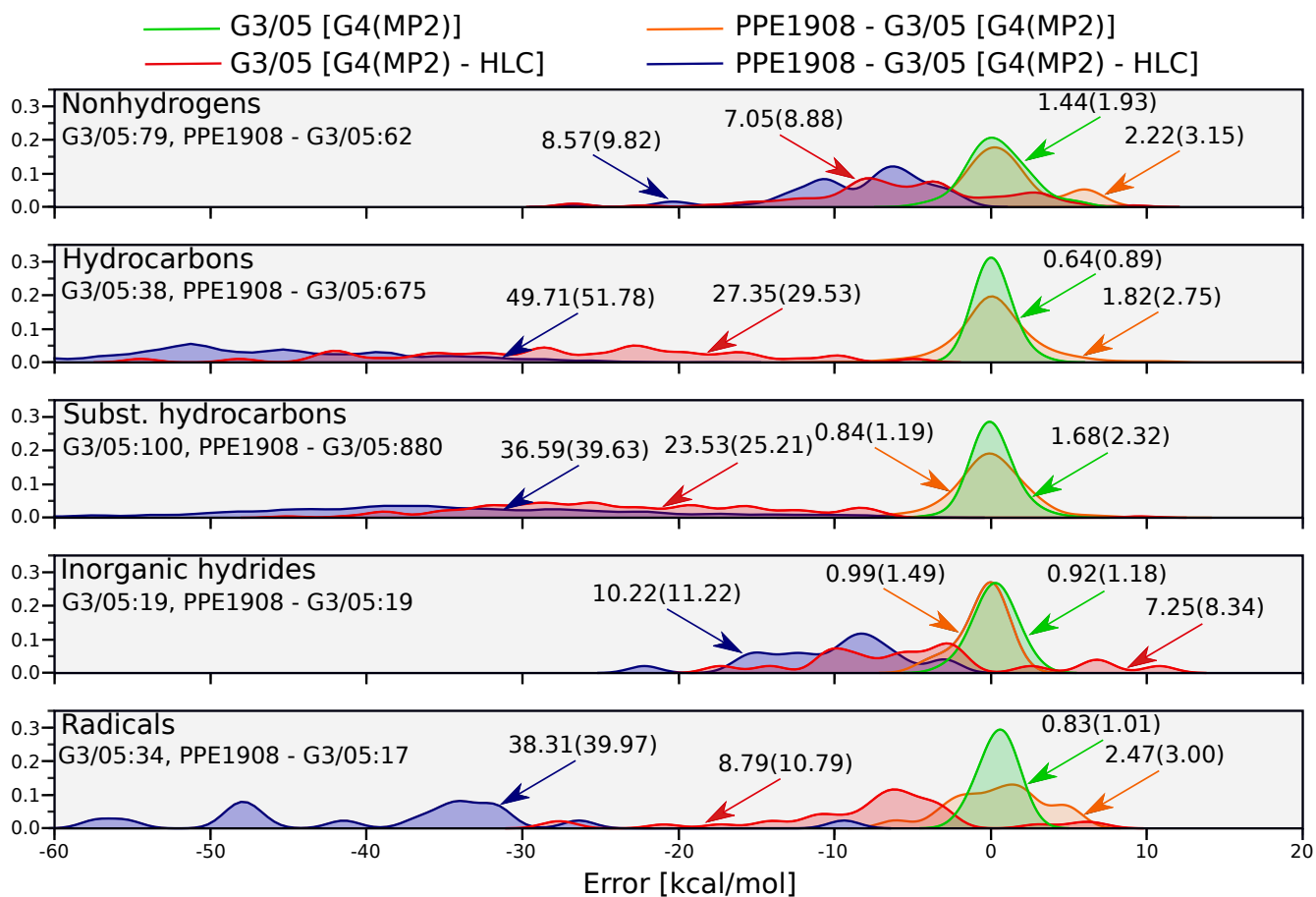


FIG. 10. Influence of HLC in determining ΔH_f° for various classes of compounds in the G3/05 dataset and rest of the compounds in the PPE1908 dataset. For both sets, results are shown separately with and without the HLC term. The arrows point to MUE (RMSE) for each error distribution. The lower bound of the error is set to -60 kcal/mol for clarity.

the error distribution to center at zero, but also changes the shape of the distribution. This indicates the HLC

term to account for both systematic and non-systematic corrections. While the contributions from ΔHF seems negligible, excluding this term in the G4(MP2) energy deteriorates the MUE for the 270 values of ΔH_f° from 0.99 kcal/mol to 1.38 kcal/mol. Reoptimizing the HLC term without the HF corrections takes the MUE to 1.16 kcal/mol, still deviating from the G4(MP2) value by 0.17 kcal/mol.

Having observed the influence of HLC on 270 ΔH_f° s in G3/05, we investigate its transferability across various classes of compounds in G3/05 and PPE1908 (Fig. 10). HLC for nonhydrogens reduces MUE \approx 4-times from the non-HLC corrected ones in G3/05 while the drop is nearly 5-fold for the remaining nonhydrogens in PPE1908. G3/05 hydrocarbons, show a \approx 43-fold decay in MUE due to HLC correction while the decay is 27-fold for the remaining ones in PPE1908. Drop in MUE is 14- and 44-fold for substituted hydrocarbons in G3/05 and the rest in PPE1908, respectively. For inorganic hydrides, MUE drops 7-fold for G3/05, while it is 11-fold for others in PPE1908. Radicals show a 10-fold decay in MUE for G3/05 while the rest in PPE1908 show a 16-fold drop. Though HLC captures systematic and non-systematic effects successfully across compound types and datasets, we do note the quantitative prediction accuracy of G4(MP2) to drop from 0.99 kcal/mol to 1.65 kcal/mol, when going from the G3/05 dataset (Table III) to the PPE1908 set (Table I). This drop in accuracy when increasing the dataset size may be ascribed to both the residual uncertainties in the experimental results, and also the systematic error introduced in the form of empirical reference data for atoms, forms the subject of Section VID.

The original motivation to add a HLC term in the G1 theory⁸⁴ is to account for the remaining basis set errors in the model. It has been noted that a successful performance of the method requires the finite basis sets employed at various levels be "balanced"⁸⁴. To probe the sensitivity of HLC to the choice of basis set, we replaced the Pople basis sets used in G4(MP2) with Dunning or Karlsruhe basis sets and re-parameterized all components in HLC by training on the G3/05 dataset; see Eq. 6 for the definitions. The resulting parameters are presented in Table IV. As expected, when moving from the default G4(MP2) basis sets to larger Karlsruhe sets (dTQ and dTQD series in Table IV), we find the magnitude of the HLC parameters to drop indicating less dependence of the accuracy on the HLC term; this trend is reminiscent of the fact that going from G4(MP2) to G4²³, the magnitude of the HLC parameters decrease. This, however, does not necessarily lead to any increase in the method's accuracy, as G4(MP2)-dTQD's MUE increases to 1.95 kcal/mol. Among the tested variants, the one using the smallest basis sets, G4(MP2)-dSTQ, shows the HLC parameters of larger magnitudes. Surprisingly, we find this variant to have an MUE of 1.22 kcal/mol, which is much smaller than that of G4(MP2)-dTQD. The

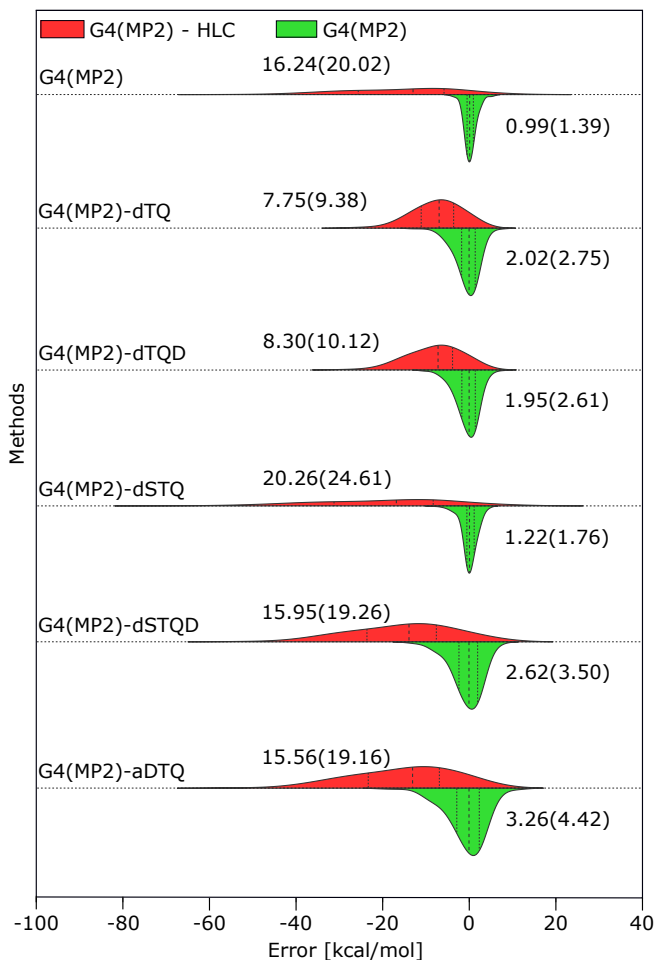


FIG. 11. Distribution of prediction errors for the G3/05 dataset, with and without reoptimized HLC. For 270 ΔH_f° values, results are shown for variants of G4(MP2) based on different basis sets. See Table IV for more details.

method suffers maximum deterioration when using the aug-cc-pVXZ basis sets, resulting in an MUE of 3.26 kcal/mol. These results indicate that successfully exploiting the form of the HLC term, also requires careful tailoring of the basis sets used for the CCSD(T), MP2 and HF energies. For the variants tried, we have presented the error distributions with and without the HLC contributions, in Fig.11.

C. ISO24 dataset for isomerization reaction energies

Accurate prediction of isomerization energies is one of the stringent tests for the reliability of WFTs, cWFTs and DFAs alike¹¹⁴. This is because isomerization reaction energetics exclusively encode information about orbital hybridization, electronic conjugation and steric effects in chemical bonding^{115,116}. Previous studies have observed majority of the DFAs to predict qualitatively incorrect trends for the energy ordering of constitutional

TABLE IV. HLC parameters for the G4(MP2) method using various basis sets trained on the G3/05 dataset. For each variant the mean unsigned error (MUE) is also given.

Method	HLC parameters (mE_H)						MUE (kcal/mol)
	A	A'	B	C	D	E	
G4(MP2)	9.472	3.102	9.741	2.115	9.769	2.379	0.99
G4(MP2)-dTQ ^a	6.18061	2.45033	5.62914	2.29326	6.41957	4.69530	2.02
G4(MP2)-dTQD ^b	5.53826	2.42024	5.10429	1.81189	5.73533	6.96434	1.95
G4(MP2)-dSTQ ^c	12.99745	3.82593	13.10205	3.37982	13.42932	-0.12345	1.22
G4(MP2)-dSTQD ^d	8.64216	2.76141	7.98680	2.32481	8.90121	3.95877	2.62
G4(MP2)-aDTQ ^e	6.85947	2.20201	6.23527	1.46485	7.11763	5.16631	3.26

^a CCSD(T)/def2-TZVP, MP2/def2-QZVP, HF/CBS(def2-TZVP,def2-QZVP)

^b CCSD(T)/def2-TZVPPD, MP2/def2-QZVPPD, HF/CBS(def2-TZVPPD,def2-QZVPPD)

^c CCSD(T)/def2-SVP, MP2/def2-TZVP, HF/CBS(def2-TZVP,def2-QZVP)

^d CCSD(T)/def2-SVPD, MP2/def2-TZVPPD, HF/CBS(def2-TZVPPD,def2-QZVPPD)

^e CCSD(T)/aug-cc-pVDZ, MP2/aug-cc-pVTZ, HF/CBS(aug-cc-pVTZ,aug-cc-pVQZ)

TABLE V. Accuracies of G4(MP2), ccCA, ω B97X-D3 and ω B97X-V for the prediction of isomerization enthalpies for 24 sets of constitutional isomers: MUE is mean unsigned error (in kcal/mol), RMSE is root-mean-square-error (in kcal/mol), and ρ is the Spearman rank correlation coefficient; the latter quantity is reported per stoichiometry.

Stoichiometry (#)	MUE (RMSE, ρ)			
	G4(MP2)	ccCA	ω B97X-D3	ω B97X-V
C ₄ H ₆ (7)	1.04 (1.21, 0.98)	0.81 (1.02, 1.00)	3.20 (3.82, 1.00)	3.56 (4.25, 1.00)
C ₅ H ₈ (8)	0.67 (0.71, 1.00)	0.22 (0.29, 1.00)	1.94 (2.46, 0.98)	2.91 (3.19, 1.00)
C ₆ H ₆ (3)	1.07 (1.64, 1.00)	1.18 (1.35, 1.00)	1.64 (1.81, 1.00)	2.12 (2.52, 1.00)
C ₆ H ₈ (6)	1.46 (1.63, 0.95)	1.14 (1.22, 0.99)	1.11 (1.49, 0.99)	1.54 (1.95, 0.99)
C ₆ H ₁₀ (8)	1.02 (1.40, 0.93)	0.78 (1.25, 0.93)	1.29 (1.67, 0.95)	1.58 (2.16, 0.95)
C ₆ H ₁₂ (19)	0.50 (0.61, 0.95)	0.61 (0.73, 0.97)	1.87 (1.98, 0.96)	3.27 (3.45, 0.98)
C ₇ H ₈ (9)	1.69 (1.98, 0.96)	1.69 (1.91, 0.96)	3.09 (3.63, 0.96)	4.20 (5.23, 0.96)
C ₇ H ₁₂ (7)	1.49 (2.06, 1.00)	1.52 (2.05, 1.00)	0.68 (0.85, 1.00)	2.00 (2.11, 1.00)
C ₇ H ₁₄ (18)	2.51 (2.59, 0.99)	2.16 (2.21, 0.99)	1.38 (1.59, 0.95)	1.31 (1.52, 0.98)
C ₈ H ₁₀ (13)	1.35 (1.60, 0.98)	1.36 (1.59, 0.98)	2.02 (2.82, 0.98)	3.43 (4.25, 0.96)
C ₈ H ₁₄ (10)	0.87 (1.12, 0.98)	0.76 (1.06, 0.96)	0.46 (0.72, 0.98)	1.61 (1.85, 0.92)
C ₉ H ₁₂ (14)	1.15 (1.64, 0.98)	0.98 (1.35, 0.98)	1.60 (2.75, 0.99)	1.91 (3.31, 0.98)
C ₁₀ H ₁₀ (7)	3.55 (3.73, 1.00)	2.92 (3.10, 1.00)	4.77 (5.76, 1.00)	4.09 (4.74, 1.00)
C ₁₀ H ₁₄ (4)	2.27 (2.69, 1.00)	1.89 (2.25, 1.00)	1.57 (2.00, 1.00)	0.73 (0.79, 1.00)
C ₁₀ H ₁₆ (9)	2.47 (3.05, 0.99)	2.97 (3.32, 0.99)	3.15 (3.45, 0.99)	5.68 (6.39, 0.99)
C ₁₂ H ₁₆ (6)	2.68 (3.04, 0.86)	2.76 (3.14, 0.86)	4.74 (5.40, 0.68)	4.68 (4.84, 0.68)
C ₆ H ₇ N (6)	0.62 (0.87, 1.00)	1.07 (1.26, 1.00)	1.39 (1.86, 1.00)	0.76 (0.97, 1.00)
C ₇ H ₉ N (7)	1.75 (2.64, 1.00)	1.72 (2.56, 1.00)	2.01 (3.39, 1.00)	1.51 (2.61, 1.00)
C ₅ H ₁₂ O (9)	0.47 (0.63, 0.99)	0.47 (0.63, 0.99)	0.83 (0.91, 0.99)	0.68 (0.74, 0.99)
C ₈ H ₁₀ O (10)	1.40 (1.48, 0.89)	1.46 (1.55, 0.89)	1.60 (1.68, 0.87)	1.72 (1.84, 0.85)
C ₅ H ₁₀ O ₂ (10)	3.55 (3.84, 0.99)	3.44 (3.76, 1.00)	3.40 (3.76, 0.96)	5.02 (5.46, 0.96)
C ₆ H ₁₂ O ₂ (9)	2.94 (3.53, 0.94)	3.36 (3.90, 0.94)	3.80 (4.35, 0.92)	3.22 (3.92, 0.92)
C ₅ H ₁₂ S (9)	0.57 (0.75, 0.95)	0.33 (0.52, 0.95)	0.91 (1.01, 0.87)	0.60 (0.68, 0.91)
C ₆ H ₁₄ S (7)	1.70 (2.22, 0.88)	1.25 (1.91, 0.79)	1.68 (1.93, 0.86)	1.34 (1.79, 0.88)
Total (215)	1.59 (2.13)	1.51 (2.05)	2.03 (2.79)	2.53 (3.39)

isomers belonging to a stoichiometry¹¹⁷. From the point of view of thermochemical procedures, all systematic contributions to molecular enthalpies such as empirical atomic corrections, and HLC are cancelled in isomerization energies. Hence, prediction errors expose non-systematic errors encoded in the evaluation of electronic energies. To identify a large benchmark suite of isomerization energies, we have collected constitutional isomers belonging to 24 unique stoichiometries in the PPE1908 dataset amounting to 239 systems.

Table V presents, for each stoichiometry, mean errors

in the prediction of isomerization energies where the reactant is the global minimum in each set, amounting to 215 reaction energies. Over the set of 215 reaction energies, we find G4(MP2) and ccCA to yield MUEs of 1.59 and 1.51 kcal/mol, respectively. Both DFAs ω B97X-V and ω B97X-D3 have performed consistently resulting in MUEs of 2–2.5 kcal/mol. All the methods considered here have also predicted the ordering of the energies of the constitutional isomers as quantified through ρ . It is interesting to see that there are sets such as C₅H₁₀O₂ for which G4(MP2) predictions show the largest discrepan-

cies, albeit preserving the energy ranking of the constitutional isomers so well with $\rho = 0.99$.

For all the global minima in the ISO-24 set, we have analyzed the computational methods' accuracies in the prediction of ΔH_f° ; the results are shown in Fig. 12. As a striking trend, one notes in spite of the errors of both DFAs staying within 3 kcal/mol, ω B97X-V consistently overstabilizes the isomers, while ω B97X-D3 mostly destabilizes these. While majority of the cWFTs' predictions show errors < 2 kcal/mol, we find G4(MP2) and ccCA to show a large discrepancy for the fused ring $C_{10}H_{10}$. It is interesting to relate these trends to the fact that such subtle discrepancies in predictions arise due to non-systematic errors, the origin of which lies in the very foundations of these electronic structure methodologies.

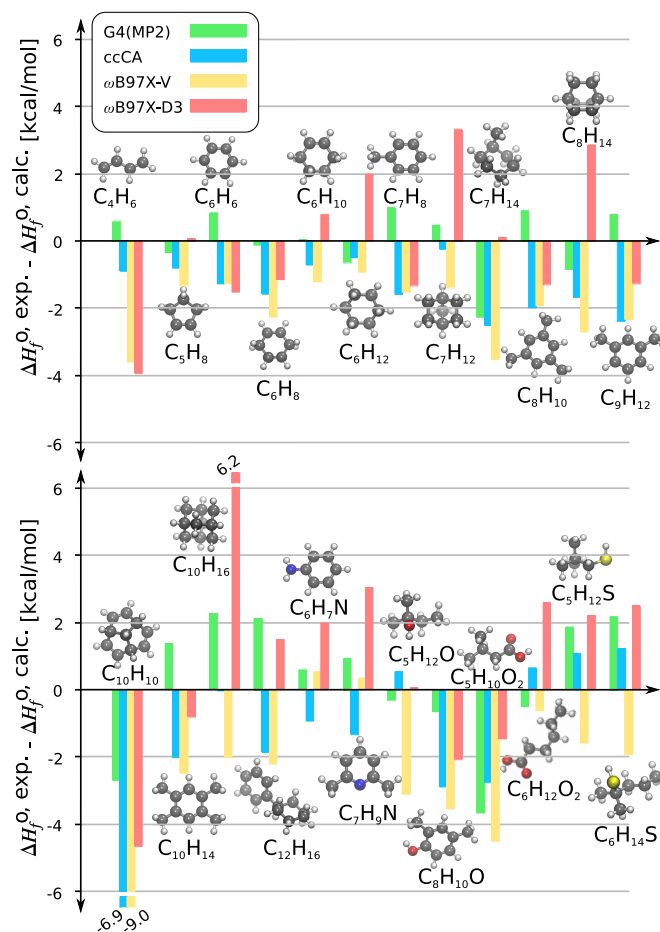


FIG. 12. Errors in G4(MP2), ccCA, ω B97X-D3 and ω B97X-V predicted ΔH_f° for every global minimum in ISO24. For each of the 24 stoichiometries, structure of the global minimum is shown.

D. Source of Systematic Errors in Molecular Standard Formation Enthalpies

Molecular $\Delta H_f^\circ(298\text{ K})$ depends on enthalpies of constituent atoms in their standard elemental forms. The absolute enthalpies per atom for the elements enter the calculation as empirical constants: $\Delta H_f^\circ(0\text{ K})$, which is the zero-Kelvin enthalpy of formation per atom along with an associated thermal correction, $H^\circ(298\text{ K}) - H^\circ(0\text{ K})$. The former quantity contributes predominantly to the total energy, hence any uncertainty in their determination will be accrued with increasing molecular size. This has been exemplified by Tasi *et al.*,¹¹⁸ for C_1 - C_{13} alkanes modelled with G2(MP2,SVP) where large systematic errors were noted when the conventional value of $\Delta H_f^\circ(0\text{ K})=169.98$ kcal/mol was used for the C atom. The re-evaluated value of 170.11 kcal/mol was shown to reduce systematic errors for that dataset. On the same note, Perdew *et al.*,¹¹⁹ have remarked on the extensive nature of the self-interaction error in spin-polarized DFAs, and their role in compromising atomization energy predictions.

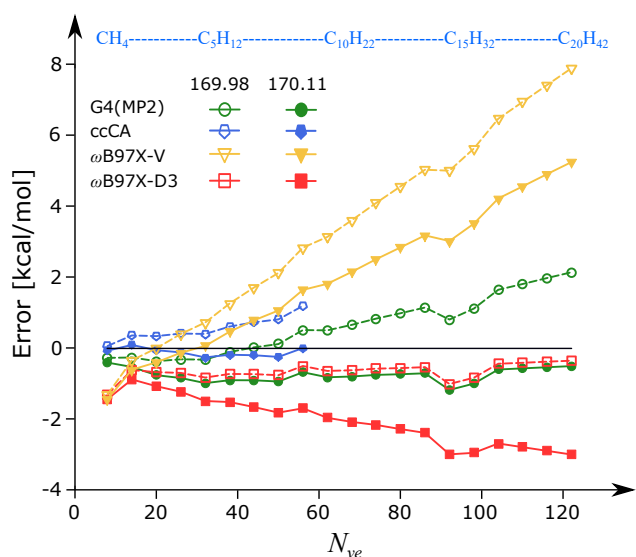


FIG. 13. Systematic errors in G4(MP2), ccCA, ω B97X-D3 and ω B97X-V predictions of ΔH_f° due to the choice of $\Delta H_f^\circ(C_{gas}, 0\text{ K})$ shown for the smallest 20 linear alkanes.

We have revisited the case of linear alkanes by increasing the set until icosane ($C_{20}H_{42}$) and modeling ΔH_f° with G4(MP2), ccCA, ω B97X-D3 and ω B97X-V. Fig. 13 displays the prediction errors for all 4 methods employing two different values for $\Delta H_f^\circ(C_{gas}, 0\text{ K})$: 169.98 kcal/mol and 170.11 kcal/mol. As a general trend, we note all deviations to drop systematically when going from the conventional parameter to the one fitted for C_1 - C_{13} alkanes. We find both G4(MP2) and ccCA to benefit from the systematic shift resulting in re-

duced prediction errors; ccCA agreeing with the experimental values for C₁-C₉ alkanes better than G4(MP2). The DFA ω B97X-V showing the maximum error among the methods considered here improves from a mean error of 3.5 kcal/mol to 2.2 kcal/mol. On the other hand, ω B97X-D3 that has shown excellent agreement with experimental values of ΔH_f° with an MUE of 0.7 kcal/mol when using the conventional $\Delta H_f^\circ(\text{C}_{\text{gas}}, 0 \text{ K})$ deteriorates by 1.4 kcal/mol when depending on the re-evaluated parameter.

VII. CONCLUSIONS

A benchmark dataset of experimental ΔH_f° for 1908 compounds that are electronically and structurally rich is presented. This dataset was assembled by collecting several previously reported benchmark suites including the ‘legacy’ dataset—G3/05 comprising 270 entries. The resulting set included 113 ‘outliers’ with potentially non-negligible experimental uncertainties detected with a probabilistic approach. The procedure also takes into consideration, uncertainties associated with the reference theory, G4(MP2). Our approach can further be refined using a reference cWFT which is more accurate than G4(MP2), albeit incurring a higher computational cost. For this purpose, the full dataset with potential outliers comprising over 2k structures and ΔH_f° have been provided in the Supplementary Information. A more robust approach would be to consider more than one high-fidelity reference methods and make a joint-probabilistic model to prune the dataset. The only tunable parameter in this model is the threshold percentile used for selecting valid benchmarks; this value was set to the 95th percentile for the reference method G4(MP2). We have adopted a bootstrapping strategy to estimate the variance in the model arising from sampling bias. Our final results are based on the lower bound for the error-threshold to mark an entry as outlier.

Along with the G4(MP2) and experimental results for the PPE1908 dataset, we have reported extensive benchmark results of formation enthalpies predicted with the cWFT ccCA, and 23 DFAs. Conventional error metrics such as MUE have been reported along with probabilistic metrics such as Q50, Q75, Q90, and Q95, that provide information about the probability and cumulative densities of errors as suggested in other studies^{106,120}. When compared to pruned experimental values, among the methods considered in this study, G4(MP2) and ccCA deliver the best performance amounting to an MUE of about 1.65 kcal/mol. The semi-empirical methods PM6 and PM7, as expected, result in rather accurate ΔH_f° with errors ≈ 5 kcal/mol. The most popular DFA, B3LYP exhibits an error of over 15 kcal/mol. However, its long-range and dispersion corrected versions, namely, CAM-B3LYP and B3LYP-D3 show errors in the 4 – 5 kcal/mol error window; in this range, we

also find the mGGA method TPSS, the global hybrid functional M06-2X and its D3 corrected variant. Dispersion corrected double hybrid functionals B2PLYP-D3 and mPW2PLYP-D show better performances with an error of 3 – 4 kcal/mol. For the prediction of ΔH_f° , we found the best performing class of DFAs to be the range-separated method ω B97X, and its modifications yielding rather accurate predictions in the error window of $\approx 2 - 3$ kcal/mol. As a general trend, we note empirical dispersion corrections to lead to a gain in prediction accuracy.

Our analysis have revealed that the original G4(MP2) method and the empirical parameterization of the HLC involved in that model retain their transferability going from the G3/05 set with 270 entries to the proposed PPE1908 set that is 7 times larger. This suggests that the prediction accuracy of G4(MP2) to hold not only for closed-shell, organic molecules of the type encountered in the QM9 dataset,^{5,30} but also to datasets with free-radicals, non-hydrogens and inorganic hydrides. As an interesting result, we find the best DFA ω B97-XV, resulting in an MUE of 2.86 kcal/mol for the $\approx 2\text{k}$ dataset, to show large systematic errors when tested on linear alkanes with 1 – 20 C atoms. This suggests that the parameters that enter into the design of this functional are somewhat overfitted to the training data with small molecules. It will be compelling to see if modern functionals can be designed by benchmarking on the diverse dataset presented here. Similarly, it will be of interest to see if cWFTs based on additional parameterization such as in the G4(MP2)-6X method¹²¹ and its variants^{122,123} preserve their transferability going from the small molecules set to the PPE1908 set.

Further, from the entire benchmark suite presented here, we have identified 24 sets of constitutional isomers; reaction enthalpies for this ISO24 dataset were benchmarked over G4(MP2), ccCA, and the two best performing DFAs. Isomerization energies are not influenced by HLC parameters, hence they present a stringent test for the prediction capabilities of methods like G4(MP2). For the prediction of 215 reaction energies, we have noted MUEs of 1.59 and 1.51 kcal/mol for G4(MP2) and ccCA. In this case, the DFAs ω B97-XD3 and ω B97-XV have also yielded excellent predictions with MUEs of $\approx 2-2.5$ kcal/mol. When extending the application of G4(MP2) method to molecules with large number of C atoms, we find the prediction accuracy to be sensitive to an empirical atomic parameter, which suggests that a careful evaluation of these parameters for all atom types is essential to prevent systematic accumulation of errors. Such calibration should be done with a method such as W4 or HEAT-456(Q) that is more robust than the method considered here. Preferably such an effort could be undertaken by pruning the total dataset and retaining only highly-precise experimental entries. Thermochemistry modeling done at such a rigour has been shown to be sensitive even to the effect anharmonicity has on molecular ZPVE^{124,125}, hence these effects must be incorpo-

rated with methods such as second-order vibrational perturbation theory (VPT2)^{126,127} that are amenable for large scale modeling.

VIII. ACKNOWLEDGEMENTS

SKD is grateful to TIFR Hyderabad for a junior research fellowship. All authors thank TIFR for support. This project was funded by intramural funds at TIFR Hyderabad from the Department of Atomic Energy (DAE). All calculations have been performed using the Helios computer cluster, which is an integral part of the MolDis Big Data facility, TIFR Hyderabad (<https://moldis.tifrh.res.in/>).

IX. DATA AVAILABILITY

The data that supports the findings of this study are available within the article and its supplementary material.

APPENDIX: EMPIRICAL THERMOCHEMISTRY PARAMETERS

TABLE VI. Heats of formation of atoms at 0 K, $\Delta H_f^\circ(0\text{ K})$, and enthalpy corrections, for elements in their standard states, $H^\circ(298\text{ K}) - H^\circ(0\text{ K})$. Unless specified, all values are taken from Ref. 128. For elements for which more than one value are available, we have utilized the more recent one marked by bold font. All values are in kcal/mol.

Atom	$\Delta H_f^\circ(0\text{ K})$	$H^\circ(298\text{ K}) - H^\circ(0\text{ K})$
H	51.63	1.01
Li	37.69	1.10
Be	76.48	0.46
B	136.2	0.29
C	169.98	0.25
N	112.53	1.04
O	58.99	1.04
F	18.47	1.05
Na	25.69	1.54
Mg	34.87	1.19
Al	78.23	1.08
Si	106.6	0.76
P	75.42	1.28
S	65.66	1.05
Cl	28.59	1.10
K	21.4830 ¹²⁹	1.6926 ¹²⁹
Ca	42.3850 ¹²⁹	1.3709 ¹²⁹
Ga	64.7633 ¹²⁹	1.3291 ¹²⁹
Br	28.1836 ¹³⁰	2.930 ^{130,131}
Ge	89.354 ¹³² , 88.2 ¹³³	1.104 ^{132,134}
As	68.86 ¹³⁵ , 68.8 ^{132,136}	1.23 ¹³⁴
Se	57.899 ¹³⁷	1.319 ¹³⁷

X. REFERENCES

- J. Cioslowski, *Quantum-mechanical prediction of thermochemical data* (Springer Science & Business Media, 2002).
- K. K. Irikura and D. J. Frurip, *Computational Thermochemistry* (ACS Publications, 1998) Chap. 1, pp. 2–18.
- O. A. von Lilienfeld, *Angew. Chem. Int. Ed.* **57**, 4164 (2018).
- R. Ramakrishnan and O. A. von Lilienfeld, *Rev. Comp. Ch.* **30**, 225 (2017).
- B. Narayanan, P. C. Redfern, R. S. Assary, and L. A. Curtiss, *Chem. Sci.* **10**, 7449 (2019).
- J. Hachmann, R. Olivares-Amaya, S. Atahan-Evrenk, C. Amador-Bedolla, R. S. Sánchez-Carrera, A. Gold-Parker, L. Vogt, A. M. Brockway, and A. Aspuru-Guzik, *J. Phys. Chem. Lett.* **2**, 2241 (2011).
- S. Chakraborty, P. Kayastha, and R. Ramakrishnan, *J. Chem. Phys.* **150**, 114106 (2019).
- J. Arús-Pous, M. Awale, D. Probst, and J.-L. Reymond, *CHIMIA* **73**, 1018 (2019).
- J. Aston, *Ind. Eng. Chem.* **34**, 514 (1942).
- H. Duus, *Ind. Eng. Chem.* **47**, 1445 (1955).
- A. S. Rodgers, *J. Phys. Chem.* **71**, 1996 (1967).
- O. V. Dorofeeva, V. P. Novikov, and D. B. Neumann, *J. Phys. Chem. Ref. Data* **30**, 475 (2001).
- L. A. Curtiss, P. C. Redfern, and D. J. Frurip, in *Reviews of Computational Chemistry*, Vol. 15, edited by K. B. Lipkowitz and D. B. Boyd (Wiley VCH, New York, 2000) pp. 147–211.
- L. A. Curtiss, P. C. Redfern, and K. Raghavachari, *WIREs Comput. Mol. Sci.* **1**, 810 (2011).
- F. Jensen, *Introduction to computational chemistry* (John Wiley & sons, 2017).
- A. Karton, *WIREs Comput. Mol. Sci.* **6**, 292 (2016).
- A. Karton, E. Rabinovich, J. M. Martin, and B. Ruscic, *J. Chem. Phys.* **125**, 144108 (2006).
- Y. J. Bomble, J. Vázquez, M. Kállay, C. Michauk, P. G. Szalay, A. G. Császár, J. Gauss, and J. F. Stanton, *J. Chem. Phys.* **125**, 064108 (2006).
- M. E. Harding, J. Vázquez, B. Ruscic, A. K. Wilson, J. Gauss, and J. F. Stanton, *J. Chem. Phys.* **128**, 114111 (2008).
- D. W. Rogers, *Heats of hydrogenation: experimental and computational hydrogen thermochemistry of organic compounds* (World Scientific: Long Island, NY, 2006).
- J. M. Martin, *Annu. Rep. Comput. Chem.* **1**, 31 (2005).
- J. Montgomery Jr, J. Ochterski, and G. Petersson, *J. Chem. Phys.* **101**, 5900 (1994).
- L. A. Curtiss, P. C. Redfern, and K. Raghavachari, *J. Chem. Phys.* **126**, 084108 (2007).
- N. J. DeYonker, T. R. Cundari, and A. K. Wilson, *J. Chem. Phys.* **124**, 114104 (2006).
- N. J. DeYonker, T. Grimes, S. Yockel, A. Dinescu, B. Mintz, T. R. Cundari, and A. K. Wilson, *J. Chem. Phys.* **125**, 104111 (2006).
- A. K. Wilson, N. J. DeYonker, and T. R. Cundari, in *Advances in the Theory of Atomic and Molecular Systems (Progress in Theoretical Chemistry and Physics)*, Vol. 19, edited by P. Piecuch, J. Maruani, G. Delgado-Barrio, and S. Wison (Springer, Netherlands, 2009) pp. 197–224.
- L. Ruddigkeit, R. Van Deursen, L. C. Blum, and J.-L. Reymond, *J. Chem. Inf. Model.* **52**, 2864 (2012).
- F. A. Faber, A. S. Christensen, B. Huang, and O. A. von Lilienfeld, *J. Chem. Phys.* **148**, 241717 (2018).
- N. Lubbers, J. S. Smith, and K. Barros, *J. Chem. Phys.* **148**, 241715 (2018).
- R. Ramakrishnan, P. O. Dral, M. Rupp, and O. A. von Lilienfeld, *Scientific Data* **1**, 140022 (2014).
- R. Ramakrishnan, P. O. Dral, M. Rupp, and O. A. von Lilienfeld, *J. Chem. Theory Comput.* **11**, 2087 (2015).
- H. Kim, J. Y. Park, and S. Choi, *Scientific Data* **6**, 109 (2019).
- L. Ward, B. Blaiszik, I. Foster, R. S. Assary, B. Narayanan, and L. Curtiss, *MRS Commun.* **9**, 891 (2019).

- ³⁴N. K. Dandu, L. Ward, R. S. Assary, P. C. Redfern, B. Narayanan, I. T. Foster, and L. A. Curtiss, *J. Phys. Chem. A* (2020), 10.1021/acs.jpca.0c01777.
- ³⁵J. Pedley, R. D. Naylor, S. P. Kirby, *et al.*, *Thermochemical data of organic compounds* (Chapman and Hall, 1986).
- ³⁶J. Pedley, *Thermochemical data and structures of organic compounds*, Vol. 1 (CRC Press, 1994).
- ³⁷L. A. Curtiss, P. C. Redfern, and K. Raghavachari, *J. Chem. Phys.* **127**, 124105 (2007).
- ³⁸N. J. DeYonker, B. R. Wilson, A. W. Pierpont, T. R. Cundari, and A. K. Wilson, *Mol. Phys.* **107**, 1107 (2009).
- ³⁹L. A. Curtiss, P. C. Redfern, and K. Raghavachari, *J. Chem. Phys.* **123**, 124107 (2005).
- ⁴⁰M. Schwilk, D. N. Tahchieva, and O. A. von Lilienfeld, arXiv preprint arXiv:2004.10600 (2020).
- ⁴¹F. Neese, *WIREs Comput. Mol. Sci.* **2**, 73 (2012).
- ⁴²F. Neese, *WIREs Comput. Mol. Sci.* **8**, e1327 (2018).
- ⁴³J. J. Stewart, *J. Mol. Model.* **13**, 1173 (2007).
- ⁴⁴J. J. Stewart, *J. Mol. Model.* **19**, 1 (2013).
- ⁴⁵J. J. Stewart, "Mopac2016," (2016), Stewart Computational Chemistry, Colorado Springs, CO, USA, Available at <http://OpenMOPAC.net>.
- ⁴⁶J. P. Perdew and K. Schmidt, in *AIP Conference Proceedings*, Vol. 577 (American Institute of Physics, 2001) pp. 1–20.
- ⁴⁷A. D. Becke, *Phys. Rev. A* **38**, 3098 (1988).
- ⁴⁸J. Perdew, J. Chevary, and S. Vosko, *Phys. Rev. B* **46**, 6671 (1992).
- ⁴⁹J. P. Perdew, K. Burke, and M. Ernzerhof, *Phys. Rev. Lett.* **78**, 1396 (1997).
- ⁵⁰A. D. Becke, *J. Chem. Phys.* **98**, 5648 (1993).
- ⁵¹A. J. Cohen and N. C. Handy, *Mol. Phys.* **99**, 607 (2001).
- ⁵²X. Xu and W. A. Goddard, *Proc. Natl. Acad. Sci. USA* **101**, 2673 (2004).
- ⁵³C. Adamo and V. Barone, *J. Chem. Phys.* **110**, 6158 (1999).
- ⁵⁴J. Tao, J. P. Perdew, V. N. Staroverov, and G. E. Scuseria, *Phys. Rev. Lett.* **91**, 146401 (2003).
- ⁵⁵S. Grimme, *J. Phys. Chem. A* **109**, 3067 (2005).
- ⁵⁶Y. Zhao and D. G. Truhlar, *Theor. Chem. Acc.* **120**, 215 (2008).
- ⁵⁷T. Yanai, D. P. Tew, and N. C. Handy, *Chem. Phys. Lett.* **393**, 51 (2004).
- ⁵⁸J.-D. Chai and M. Head-Gordon, *Phys. Chem. Chem. Phys.* **10**, 6615 (2008).
- ⁵⁹N. Mardirossian and M. Head-Gordon, *Phys. Chem. Chem. Phys.* **16**, 9904 (2014).
- ⁶⁰N. Mardirossian and M. Head-Gordon, *J. Chem. Phys.* **144**, 214110 (2016).
- ⁶¹S. Grimme, S. Ehrlich, and L. Goerigk, *J. Comp. Chem.* **32**, 1456 (2011).
- ⁶²A. D. Becke and E. R. Johnson, *J. Chem. Phys.* **123**, 154101 (2005).
- ⁶³E. R. Johnson and A. D. Becke, *J. Chem. Phys.* **123**, 024101 (2005).
- ⁶⁴E. R. Johnson and A. D. Becke, *J. Chem. Phys.* **124**, 174104 (2006).
- ⁶⁵S. Grimme, *J. Chem. Phys.* **124**, 034108 (2006).
- ⁶⁶S. Grimme, J. Antony, S. Ehrlich, and H. Krieg, *J. Chem. Phys.* **132**, 154104 (2010).
- ⁶⁷T. Schwabe and S. Grimme, *Phys. Chem. Chem. Phys.* **9**, 3397 (2007).
- ⁶⁸P. Linstrom and E. W.G. Mallard, "NIST chemistry webbook, NIST Standard Reference Database Number 69, National Institute of Standards and Technology, Gaithersburg MD, 20899," (2020), (Accessed December 2019).
- ⁶⁹H. E. Pence and A. Williams, "Chemspider: An online chemical information resource," (2010), (Accessed December 2019).
- ⁷⁰S. Kim, J. Chen, T. Cheng, A. Gindulyte, J. He, S. He, Q. Li, B. A. Shoemaker, P. A. Thiessen, B. Yu, *et al.*, *Nucleic Acids Res.* **47**, D1102 (2019).
- ⁷¹M. D. Hanwell, D. E. Curtis, D. C. Lonie, T. Vandermeersch, E. Zurek, and G. R. Hutchison, *J. Cheminform* **4**, 17 (2012).
- ⁷²A. K. Rappé, C. J. Casewit, K. Colwell, W. A. Goddard III, and W. M. Skiff, *J. Am. Chem. Soc.* **114**, 10024 (1992).
- ⁷³F. Weigend and R. Ahlrichs, *Phys. Chem. Chem. Phys.* **7**, 3297 (2005).
- ⁷⁴J. W. Ochterski, *Thermochemistry in gaussian*, www.gaussian.com (2000), (Accessed December 2019).
- ⁷⁵Note that in Table I of Ref. 77 SeH⁺ has to be SeH.
- ⁷⁶L. A. Curtiss, M. P. McGrath, J.-P. Blaudeau, N. E. Davis, R. C. Binning Jr, and L. Radom, *J. Chem. Phys.* **103**, 6104 (1995).
- ⁷⁷L. A. Curtiss, P. C. Redfern, V. Rassolov, G. Kedziora, and J. A. Pople, *J. Chem. Phys.* **114**, 9287 (2001).
- ⁷⁸N. L. Allinger, J. T. Fermann, W. D. Allen, and H. F. Schaefer III, *J. Chem. Phys.* **106**, 5143 (1997).
- ⁷⁹L. A. Curtiss, K. Raghavachari, P. C. Redfern, V. Rassolov, and J. A. Pople, *J. Chem. Phys.* **109**, 7764 (1998).
- ⁸⁰J. M. Martin, *Theor. Chem. Acc.* **97**, 227 (1997).
- ⁸¹J. M. Martin, *Chem. Phys. Lett.* **259**, 669 (1996).
- ⁸²J. Martin, *J. Chem. Phys.* **97**, 5012 (1992).
- ⁸³J. M. Martin, *J. Chem. Phys.* **100**, 8186 (1994).
- ⁸⁴J. A. Pople, M. Head-Gordon, D. J. Fox, K. Raghavachari, and L. A. Curtiss, *J. Chem. Phys.* **90**, 5622 (1989).
- ⁸⁵L. A. Curtiss, K. Raghavachari, G. W. Trucks, and J. A. Pople, *J. Chem. Phys.* **94**, 7221 (1991).
- ⁸⁶N. J. DeYonker, T. G. Williams, A. E. Imel, T. R. Cundari, and A. K. Wilson, *J. Chem. Phys.* **131**, 024106 (2009).
- ⁸⁷M. L. Laury, N. J. DeYonker, W. Jiang, and A. K. Wilson, *J. Chem. Phys.* **135**, 214103 (2011).
- ⁸⁸C. Peterson, D. Penchoff, and A. Wilson, in *Annual Reports in Computational Chemistry*, Vol. 12 (Elsevier, 2016) pp. 3–45.
- ⁸⁹B. A. Hess, *Phys. Rev. A* **32**, 756 (1985).
- ⁹⁰B. A. Hess, *Phys. Rev. A* **33**, 3742 (1986).
- ⁹¹G. Jansen and B. A. Hess, *Phys. Rev. A* **39**, 6016 (1989).
- ⁹²M. Reiher, *WIREs Comput. Mol. Sci.* **2**, 139 (2012).
- ⁹³N. J. DeYonker, K. A. Peterson, G. Steyl, A. K. Wilson, and T. R. Cundari, *J. Phys. Chem. A* **111**, 11269 (2007).
- ⁹⁴T. H. Dunning Jr, K. A. Peterson, and A. K. Wilson, *J. Chem. Phys.* **114**, 9244 (2001).
- ⁹⁵N. J. DeYonker, B. Mintz, T. R. Cundari, and A. K. Wilson, *J. Chem. Theory Comput.* **4**, 328 (2008).
- ⁹⁶M. M. Ghahremanpour, P. J. Van Maaren, and D. Van Der Spoel, *Scientific Data* **5**, 180062 (2018).
- ⁹⁷P. R. Schreiner, A. A. Fokin, R. A. Pascal, and A. de Meijere, *Org. Lett.* **8**, 3635 (2006).
- ⁹⁸A. Sengupta and K. Raghavachari, *J. Chem. Theory Comput.* **10**, 4342 (2014).
- ⁹⁹O. V. Dorofeeva and M. A. Filimonova, *J. Chem. Thermodyn.* **126**, 31 (2018).
- ¹⁰⁰E. Paulechka and A. Kazakov, *J. Phys. Chem. A* **121**, 4379 (2017).
- ¹⁰¹B. Ruscic, *Int. J. Quantum Chem.* **114**, 1097 (2014).
- ¹⁰²G. N. Simm, J. Proppe, and M. Reiher, *CHIMIA* **71**, 202 (2017).
- ¹⁰³P. Pernot and A. Savin, *J. Chem. Phys.* **148**, 241707 (2018).
- ¹⁰⁴A. J. Thakkar and T. Wu, *J. Chem. Phys.* **143**, 144302 (2015).
- ¹⁰⁵T. Wu, Y. N. Kalugina, and A. J. Thakkar, *Chem. Phys. Lett.* **635**, 257 (2015).
- ¹⁰⁶P. Pernot and A. Savin, *J. Chem. Phys.* **152**, 164108 (2020).
- ¹⁰⁷A. Savin and E. R. Johnson, "Judging density-functional approximations: Some pitfalls of statistics," in *Density Functionals: Thermochemistry*, edited by E. R. Johnson (Springer International Publishing, Cham, 2015) pp. 81–95.
- ¹⁰⁸J. P. Perdew, J. Sun, A. J. Garza, and G. E. Scuseria, *Z. Phys. Chem.* **230**, 737 (2016).
- ¹⁰⁹A. Gramacki, *Nonparametric kernel density estimation and its computational aspects* (Springer, 2018).
- ¹¹⁰M. Jaidann, S. Roy, H. Abou-Rachid, and L.-S. Lussier, *J. Hazard. Mater.* **176**, 165 (2010).
- ¹¹¹L. Türker, S. Gümüş, and T. Atalar, *J. Energ. Mater.* **28**, 139 (2010).
- ¹¹²J. P. Guthrie, *J. Phys. Chem. A* **105**, 9196 (2001).
- ¹¹³C. Spearman, *Am. J. Psychol.* **15**, 72 (1904), Reprinted: *Int. J. Epidemiol.* 2010;39:113750.
- ¹¹⁴S. Grimme, M. Steinmetz, and M. Korth, *J. Org. Chem.* **72**, 2118 (2007).
- ¹¹⁵S. Luo, Y. Zhao, and D. G. Truhlar, *Phys. Chem. Chem. Phys.* **13**, 13683 (2011).

- ¹¹⁶K. W. Sattelmeyer, J. Tirado-Rives, and W. L. Jorgensen, *J. Phys. Chem. A* **110**, 13551 (2006).
- ¹¹⁷A. Karton and J. M. Martin, *Mol. Phys.* **110**, 2477 (2012).
- ¹¹⁸G. Tasi, R. Izsák, G. Matisz, A. G. Császár, M. Kállay, B. Ruscic, and J. F. Stanton, *ChemPhysChem* **7**, 1664 (2006).
- ¹¹⁹J. P. Perdew, J. Sun, A. Ruzsinszky, P. D. Mezei, and G. I. Csonka, *Period. Polytech. Chem. Eng.* **60**, 2 (2016).
- ¹²⁰P. Pernot, B. Huang, and A. Savin, arXiv preprint arXiv:2004.02524 (2020), 10.1088/2632-2153/aba184.
- ¹²¹B. Chan, J. Deng, and L. Radom, *J. Chem. Theory Comput.* **7**, 112 (2010).
- ¹²²B. Chan, A. Karton, and K. Raghavachari, *J. Chem. Theory Comput.* **15**, 4478 (2019).
- ¹²³E. Semidalas and J. M. Martin, *J. Chem. Theory Comput.* (2020), 10.1021/acs.jctc.0c00189.
- ¹²⁴F. Pfeiffer, G. Rauhut, D. Feller, and K. A. Peterson, *J. Chem. Phys.* **138**, 044311 (2013).
- ¹²⁵K. A. Peterson, D. Feller, and D. A. Dixon, *Theor. Chem. Acc.* **131**, 1079 (2012).
- ¹²⁶V. Barone, *J. Chem. Phys.* **122**, 014108 (2005).
- ¹²⁷R. Ramakrishnan and G. Rauhut, *J. Chem. Phys.* **142**, 154118 (2015).
- ¹²⁸L. A. Curtiss, K. Raghavachari, P. C. Redfern, and J. A. Pople, *J. Chem. Phys.* **106**, 1063 (1997).
- ¹²⁹M. Chase, C. Davies, J. Downey, D. Frurip, R. McDonald, and A. Syverud, "NIST-JANAF Thermochemical Tables (ver. 1.0), online, standard reference data program; national institute of standards and technology: Gaithersburg, md, usa, 1985,".
- ¹³⁰D. Trogolo and J. S. Arey, *Phys. Chem. Chem. Phys.* **17**, 3584 (2015).
- ¹³¹J. Cox, D. D. Wagman, and V. A. Medvedev, *CODATA key values for thermodynamics* (Chem/Mats-Sci/E, 1989).
- ¹³²P. M. Mayer, J.-F. Gal, and L. Radom, *Int. J. Mass Spectrom. Ion Processes* **167**, 689 (1997).
- ¹³³B. Ruscic, M. Schwarz, and J. Berkowitz, *J. Chem. Phys.* **92**, 1865 (1990).
- ¹³⁴D. Wagman, W. Evans, V. Parker, and R. Schumm, *J. Phys. Chem. Ref. Data* **11** (1982).
- ¹³⁵D. Feller, M. Vasiliu, D. J. Grant, and D. A. Dixon, *J. Phys. Chem. A* **115**, 14667 (2011).
- ¹³⁶R. Binning Jr and L. A. Curtiss, *J. Chem. Phys.* **92**, 1860 (1990).
- ¹³⁷L. Wang, *Int. J. Mass Spectrom.* **264**, 84 (2007).